ARTICLE
Journal of Cellular Biochemistry 114:2753–2769 (2013)

Journal of Cellular Biochemistry

Transglutaminase-2 Mediates Calcium-Regulated Crosslinking of the Y-Box 1 (YB-1) Translation-Regulatory Protein in TGFβ1-Activated Myofibroblasts

William L. Willis, Seethalakshmi Hariharan, Jason J. David, and Arthur Roger Strauch*

Department of Physiology and Cell Biology, The Integrated Biomedical Sciences Graduate Program, and the Ohio State Biochemistry Program, Dorothy M. Davis Heart and Lung Research Institute, College of Medicine, The Ohio State University, Columbus, Ohio, 43210

ABSTRACT

Myofibroblast differentiation is required for wound healing and accompanied by activation of smooth muscle α-actin (SMαA) gene expression. The stress-response protein, Y-box binding protein-1 (YB-1) binds SMαA mRNA and regulates its translational activity. Activation of SMαA gene expression in human pulmonary myofibroblasts by TGFβ1 was associated with formation of denaturation-resistant YB-1 oligomers with selective affinity for a known translation-silencer sequence in SMαA mRNA. We have determined that YB-1 is a substrate for the protein-crosslinking enzyme transglutaminase 2 (TG2) that catalyzes calcium-dependent formation of covalent γ-glutamyl-isopeptide linkages in response to reactive oxygen signaling. TG2 transamidation reactions using intact cells, cell lysates, and recombinant YB-1 revealed covalent crosslinking of the 50 kDa YB-1 polypeptide into protein oligomers that were distributed during SDS–PAGE over a 75–250 kDa size range. In vitro YB-1 transamidation required nanomolar levels of calcium and was enhanced by the presence of SMαA mRNA. In human pulmonary fibroblasts, YB-1 crosslinking was inhibited by (a) anti-oxidant cystamine, (b) the reactive-oxygen antagonist, diphenyleneiodonium, (c) competitive inhibition of TG2 transamidation using the aminyl-surrogate substrate, monodansylcadaverine, and (d) transfection with small-interfering RNA specific for human TG2 mRNA. YB-1 crosslinking was partially reversible as a function of oligomer-substrate availability and TG2 enzyme concentration. Intracellular calcium accumulation and peroxidative stress in injury-activated myofibroblasts may govern SMαA mRNA translational activity during wound healing via TG2-mediated crosslinking of the YB-1 mRNA-binding protein. J. Cell. Biochem. 114: 2753–2769, 2013.

KEY WORDS: MYOFIBROBLAST; YB-1; TRANSGLUTAMINASE 2; TRANSLATIONAL CONTROL; RNA-BINDING PROTEIN

The role of TGFβ1 receptor signaling is well known in the capacity of initiating the earliest cellular responses to tissue injury that, if poorly regulated, can lead to chronic myofibroblast differentiation and dysfunctional cardiopulmonary fibrosis [Gabbiani, 2003; Grotendorst et al., 2004; Frangogiannis, 2006; Willis and Borok, 2007; Liu et al., 2009; Strauch and Hariharan, 2013]. Inflammatory cells release proteases at sites of tissue damage with resultant activation of latent TGFβ1 deposited at extracellular sites during platelet de-granulation and thrombosis. Subsequent phosphorylation and nuclear translocation of canonical TGFβ1 receptor-regulated Smad proteins initiates myofibroblast differentiation including transcriptional activation of genes encoding smooth muscle α-actin [Subramanian et al., 2004; Zhang et al., 2005; Liu et al., 2009; Strauch and Hariharan, 2013] and the α1 and α2 subunits of type I collagen [Norman et al., 2001; Higashi et al., 2003; Small et al., 2010] required for assembly of an actomyosin-based contractile apparatus, efficient wound closure, and repair of damage to the extracellular matrix needed for restoring tissue structure and function. Signaling provided by non-canonical signaling downstream from TGFβ1 receptor activation including Akt and p38-MAP kinases can augment SMαA gene transcription via the calcium-regulated NFAT transcription factor [Bosc et al., 2005; Nishida et al., 2007; Davis et al., 2012]. Moreover, polymerization of

Grant sponsor: NIH NHLBI; Grant numbers: HL 085109, HL 110802; Grant sponsor: Cardiovascular Medical Research and Education Fund (CMREF).

*Correspondence: Arthur Roger Strauch, PhD, Department of Physiology & Cell Biology, Dorothy M. Davis Heart & Lung Research Institute, The Ohio State University College of Medicine, 460 West 12th Avenue, BRT 314, Columbus, OH 43210. E-mail: strauch.1@osu.edu

Manuscript Received: 19 April 2013; Manuscript Accepted: 25 June 2013

Accepted manuscript online in Wiley Online Library (wileyonlinelibrary.com): 27 June 2013

DOI 10.1002/jcb.24624 • © 2013 Wiley Periodicals, Inc.

the filamentous SMαA cytoskeleton from G-actin monomers further augments gene activation in myofibroblasts by fostering nuclear uptake of the MRTF-A transcriptional co-activator protein that dissociates from G-actin during F-actin assembly and potentiates SRF binding and transcriptional activation at several CArG box DNA-sequence motifs in the SMαA promoter [Elberg et al., 2008; Masszi et al., 2010; Small et al., 2010; Strauch and Hariharan, 2013].

Recent reports indicate an emerging role for Y-box binding protein 1 (YB-1) in governing SMαA and type I collagen mRNA stability, transport, and translational efficiency in the context of TGFβ1-mediated fibrosis and maladaptive tissue remodeling in the heart, lung, liver, and kidney [Subramanian et al., 2002; Zhang et al., 2005, 2008; Dooley et al., 2006; Fraser et al., 2008; Hanssen et al., 2011]. Thrombin and non-canonical TGFβ1 receptor-mediated activation of MEK1/Erk1,2 signaling in human pulmonary myofibroblasts disrupts the physical interaction between YB-1 and a translation-silencer sequence in exon 3 of SMαA mRNA resulting in a rapid and self-limiting burst of SMαA protein synthesis [Kelm et al., 1999b; Zhang et al., 2005]. In the cytosol, YB-1 also binds actin filaments and microtubules [Chernov et al., 2008] and accumulates proximal to cardiac intercalated discs following heart transplant [David et al., 2012]. Deposition of ribonucleoprotein complexes of YB-1 and mRNAs at polyribosomes located at cardiac intercalated discs may re-program protein synthesis required for allograft surgical healing, metabolic adaptation, and host tolerance. YB-1 is an evolutionarily conserved member of the ancient Y-box protein family containing a cold-shock domain (CSD) that exhibits high-affinity binding to single-strand nucleic acid [Wolffe, 1994; Kohno et al., 2003; Evdokimova et al., 2006]. YB-1 unwinds duplex DNA and regulates transcriptional activity of several genes associated with inflammation, fibrosis, cell proliferation, tumor cell metastasis, and epithelial–mesenchymal transition [David et al., 2012]. YB-1 also binds stem-loop structures in mRNAs encoding proteins needed for cell survival and recently was identified in cytoplasmic granules with possible functional importance in controlling mRNA stability, intracellular transport, and translational activity during peroxidative stress [Nekrasov et al., 2003; Skabkin et al., 2004; Yang and Bloch, 2007; Chernov et al., 2008; Onishi et al., 2008]. YB-1 may facilitate cellular adaptation to metabolic stress by reducing the energy demand associated with the synthesis of numerous highly specialized proteins while favoring translation of an essential sub-set of mRNAs needed for basic cell survival [Keene, 2007; Yamasaki and Anderson, 2008].

In this report we show that increased expression of SMαA protein during TGFβ1-induced myofibroblast differentiation was associated with the formation of YB-1 oligomers exhibiting SMαA mRNA-binding activity. YB-1 oligomers showed high resistance to dispersal during denaturing SDS–PAGE suggestive of covalent protein cross-linking. We determined that YB-1 is a substrate for the crosslinking enzyme, transglutaminase 2 (TG2), a ubiquitous member of the protein-glutamine γ-glutamyltransferases enzyme family (EC 2.3.2.13) with mechanistic importance in aging, myocardial hypertrophy, vascular compliance, kidney and pulmonary fibrosis, and wound healing [Stephens et al., 2004; Stamnaes et al., 2008, 2010; Iismaa et al., 2009; Kiraly et al., 2009; Mehta et al., 2010; Park et al., 2010; Santhanam et al., 2010; Lin et al., 2011; Olsen et al., 2011; Gundemir et al., 2012]. TG2 catalyzes the calcium-dependent formation of covalent γ-glutamyl-isopeptide linkages via a trans-amidation reaction in response to peroxidative stress [Stamnaes et al., 2008, 2010]. Importantly, intracellular TG2 mediates fibrogenesis downstream from TGFβ1 signaling in fibroblasts pointing to its potential importance in the molecular etiology of chronic fibrotic diseases that cause irreversible cardiopulmonary remodeling [Oh et al., 2011]. Transamidation reactions using purified recombinant protein, intact human pulmonary fibroblasts, and fibroblast lysates, revealed that YB-1 was an authentic TG2 substrate and that protein-crosslinking activity was calcium-concentration dependent and enhanced by inclusion of an oligonucleotide encompassing the exon 3 YB-1 binding site that mediates translational control of SMαA mRNA. Notably, the YB-1 crosslinking reaction was partly reversible via the known intrinsic isopeptidease activity of TG2 suggesting that YB-1 oligomer formation and dissolution may be dynamic, metabolically regulated events during myofibroblast differentiation.

MATERIALS AND METHODS

CELL CULTURE METHODS AND PREPARATION OF PROTEIN EXTRACTS

Human pulmonary fibroblasts (hPFB) were established in primary culture from enzyme-dispersed tissue fragments of human neonatal lung tissue obtained at autopsy and were kindly provided by Dr. Daren L. Knoell (Departments of Pharmacy and Internal Medicine, The Ohio State University, Columbus, OH). Pulmonary fibroblasts were maintained in a 1:1 mixture of Ham′s F-12 and DMEM (1.0 g/L D-glucose) supplemented with penicillin-streptomycin-Fungizone™, Gentamicin™ (50 μg/ml), and 10% heat-inactivated fetal bovine serum (hiFBS; Invitrogen, Carlsbad, CA). Human pulmonary artery adventitial fibroblasts (PAAFs) established in primary culture from artery explants obtained at autopsy were provided by the Pulmonary Hypertension Breakthrough Initiative (Ann Arbor, MI). PAAFs were cultivated in defined medium SmGM2 containing 5% hiFBS (Lonza, Walkersville, MD). Cell preparations were cultivated in a humidified incubator at 37°C at 5% CO_2 and were rendered quiescent by a 48 h exposure to HEPES-buffered DMEM (1.0 g/L D-glucose) containing 0.5% hiFBS and penicillin-streptomycin-Fungizone™. Recombinant human TGFβ1 (rhTGFβ1, 5 ng/ml, final concentration; R &D Systems, Minneapolis, MN) was added to cultures for varying periods before preparation of protein extracts. Human plasma thrombin (1,000 NIH U/mg protein) was obtained from Calbiochem (La Jolla, CA) and used at a final concentration of 5 U/ml [Zhang et al., 2005]. Right ventricular septal endomyocardial biopsies were retrieved under aseptic conditions from participating patients providing informed written consent. As previously reported, biopsies were collected in the cardiac catheterization laboratory in the Ross Heart Hospital, The Ohio State University Medical Center and processed for protein extracts in accordance with IRB-approved protocols [David et al., 2012].

To prepare nuclear and cytosolic protein extracts, cell monolayers were washed twice with Dulbecco′s phosphate-buffered saline (PBS), scraped into fresh PBS, sedimented at 3,000 rpm, washed once more in PBS, and resuspended in 400 μl of hypotonic buffer (10 mM

HEPES, pH 7.9, 1.5 mM $MgCl_2$, 10 mM KCl, 0.2 mM EDTA, 0.2 mM phenylmethylsulfonyl fluoride [PMSF], and 0.5 mM dithiothreitol [DTT]). Cells were allowed to swell on ice for 15 min followed by the addition of 25 μl of a 10% solution of Nonidet™ NP-40 and vigorous vortexing for 10 s to rupture the cells and release nuclei that were then collected by centrifugation at 4°C. Supernatants containing the cytosol fraction were reserved and stored at −80°C. Nuclei were re-suspended in 1/2 packed-pellet volume of ice-cold, low-salt buffer (20 mM HEPES, pH 7.9, 25% glycerol, 1.5 mM $MgCl_2$, 20 mM KCl, 0.2 mM EDTA, 0.2 mM PMSF, 0.5 mM DTT). High salt buffer (20 mM HEPES, pH 7.9, 25% glycerol, 1.5 mM $MgCl_2$, 1.2 M KCl, 0.2 mM EDTA, 0.2 mM PMSF, and 0.5 mM DTT) equal to 1/2 packed-pellet volume was added and the nuclei further extracted with gentle rocking for 20 min at 4°C. Nuclear debris was removed by a 30 min centrifugation at 14,500 rpm at 4°C and the supernatant immediately desalted by buffer-exchange with low-salt buffer using a 0.5 ml capacity 10,000 MWCO Amicon centrifugal-microfiltration device (Millipore, Billerica, MA). To prepare RIPA (whole cell) extracts, PBS-washed fibroblasts were scraped from culture vessels into PBS, sedimented at 3,000 rpm, washed once in PBS, and extracted in 200 μl of RIPA buffer (50 mM Tris-HCl, pH 8.0, 1% NP-40, 0.5% sodium deoxycholate, 0.1% SDS, protease inhibitor cocktail, 0.2 mM PMSF, and 1 mM DTT) for 30 min on ice. RIPA extracts were clarified by centrifugation at 14,500 rpm for 30 min at 4°C and the resulting supernatant stored at −80°C.

RNA-BINDING ASSAYS

The following synthetic biotinylated oligonucleotide probes (Integrated DNA Technologies, Coralville, IA) were used in this study: (1) a 30-nt RNA-coding element from exon 3 of SMαA mRNA (CE-RNA, gggaguaaugguuggaaugggccaaaaaga), previously shown to bind YB-1 and Pur proteins [Kelm et al., 1999b], (2) a 25-nt sequence containing a cold-shock domain-like consensus (underlined text) from exon 9 of SMαA mRNA (CSD1, gaucgguggc**uccauc**uuggcuucgc), (3) a 25-nt sequence containing a cold-shock domain-like consensus motif (underlined text) from exon 8 of SMαA mRNA (CSD4, gcauccacga**aac-cac**cuauaacagc), and (4) a 25-nt sequence encompassing an MCAT-like sequence (underlined text) from the 3′untranslated region of SMαA mRNA (3′UTR, 5′-uuuccaaau**cauuccu**agccaaagcu-3′). RNA-binding reactions containing either RIPA or nuclear protein extracts (100 μg) combined with each of the above biotinylated oligonucleotides (100 pmol) were incubated in a buffer containing 5 μg/ml poly(dI-dC), 10 mM Tris, pH 7.5, 50 mM NaCl, 0.5 mM DTT, 0.5 mM EDTA, 0.12 mM PMSF, 4% glycerol. Protein/RNA complexes were captured during a 30 min incubation with streptavidin-immobilized paramagnetic beads (Promega, Madison, WI; 0.6 ml bead suspension/reaction) as described previously [Cogan et al., 2002; Subramanian et al., 2004; Zhang et al., 2008]. After washing four times with buffer containing 25 mM Tris-HCl, pH 7.5, 1 mM EDTA, and 100 mM NaCl, bound protein was eluted using one packed-bead volume of 2× protein-denaturing buffer and analyzed by SDS–PAGE and immunoblot procedures.

IMMUNOBLOT PROCEDURES

Proteins were size-fractionated by SDS–PAGE on 10% polyacrylamide gels and electrophoretically transferred to nitrocellulose membranes. Standard protein transfers were performed overnight at a constant 45 mA using a TE22 electrophoretic transfer apparatus (Hoefer, Inc., Holliston, MA) and a transfer buffer containing 25 mM Tris, 190 mM glycine, 20% methanol. For high-efficiency transfer of high molecular weight YB-1 oligomers, selected gels were transferred to membranes using a slightly modified method employing a single-use transfer buffer containing 48 mM Tris, 390 mM glycine, 0.05% SDS, and 20% methanol and two-stage electrophoresis process (60 mA for 16 h followed by 450 mA for an additional 3 h). After overnight blocking at 4°C in Tris-buffered saline (TBS; 25 mM Tris-HCl, pH 7.5, and 150 mM NaCl) containing 0.1% (v/v) Tween 20™ and 5% (w/v) bovine serum albumin (BSA), transfer membranes were incubated with selected rabbit polyclonal antibodies (1–2 μg/ml) overnight at 4°C with gentle rocking. Blots were washed four times at room temperature over a 20-min period in TBS containing 0.3% (v/v) Tween 20™, incubated with horseradish peroxidase-conjugated, goat anti-rabbit secondary antibody for 45 min, washed, and processed for development of a chemiluminescence-emission signal that was detected using a ChemiDoc™ XRS CCD-imaging camera (BioRad, Hercules, CA). Chemiluminescence image-capture times were varied over a period of 30–500 s to distinctly resolve the p50 and p75–250 weight regions on YB-1 immunoblots that are depicted in some figures as separate digital-image components. Antibodies for detection of human transglutaminase 2 were obtained from Cell Signaling Technology (Beverly, MA). YB-1-specific rabbit polyclonal antibodies M85–110 and M276–302 are reactive with the YB-1 CSD and C-terminal regions, respectively, and were kindly provided by Dr. Robert J. Kelm, Jr., in the Department of Medicine, Cardiovascular Research Center, at the University of Vermont [Kelm et al., 1999a]. Additional rabbit polyclonal antibodies specific for either N- or C-terminal portions of YB-1 were obtained from Sigma-Aldrich (St. Louis, MO) and an anti-histidine antibody (RGSHHHH anti-HIS mouse IgG1 monoclonal antibody) used to detect recombinant N-His YB-1 (see below) in crosslinking reactions was obtained from Qiagen Sciences (Germantown, MD).

PURIFICATION OF RECOMBINANT N-HIS YB-1

Expression of recombinant N-terminal hexahistidine-tagged mouse YB-1 (N-HisYB-1) in *Escherichia coli* was performed as described in Knapp et al. [2006] and Kelm et al. [1999a]. Bacterial cell pellets weighing approximately 1 g were suspended in Xtractor™ lysis buffer (Clonetech, Mountainview, CA) supplemented with 1 mg/ml lysozyme, 5 U/ml DNase, 5 U/ml RNase, 10 mM β-mercaptoethanol, 0.1 mM PMSF, and protease inhibitor cocktail. The cell suspension was incubated at room temperature for 30 min with gentle agitation. Lysates were cooled on ice for 5 min followed by sonication with a Misonix Microson XL 2000 sonicator (setting 10) for a total of six 10-s bursts with 1-min incubations on ice between bursts. Lysates were clarified by centrifugation at 14,000*g* for 20 min at 4°C and incubated in 1 ml Talon metal-affinity resin (Clontech) for 20 min at room temperature with gentle agitation. Resin-bound protein was sedimented at 700*g* for 5 min and washed with 20-bed volumes of wash buffer (50 mM sodium phosphate, pH 7.4, 300 mM NaCl, 5 mM β-mercaptoethanol, 0.1 mM PMSF, protease inhibitor cocktail). Washed resin then was resuspended in 1-bed volume of wash buffer and transferred to a 2 ml gravity-flow column, washed in 14-bed volumes wash buffer, followed by a second wash in 7-bed volumes of

wash buffer supplemented with 10 mM imidazole. Bound recombinant N-HisYB1 was eluted from the resin using 5-bed volumes of wash buffer containing 150 mM imidazole and concentrated in a centrifugation-filter device (Ultracel 10 K, Millipore). The relative purity of N-HisYB-1-containing fractions was assessed by Coomassie Fluor-Orange (Invitrogen) staining and SDS–PAGE immunoblot analysis of protein eluate using the RGSHHHH anti-HIS mouse IgG1 monoclonal antibody.

TRANSGLUTAMINASE 2-MEDIATED YB-1 CROSSLINKING REACTIONS

For crosslinking assays using endogenous YB-1 as substrate, 50 μg aliquots of RIPA whole-cell extracts prepared from human pulmonary fibroblasts were incubated in a transglutaminase 2 (TG2) reaction buffer (50 mM Tris, pH 8.0, 150 mM NaCl, 0.2 mM PMSF, 1 mM DTT, and protease inhibitor cocktail) with the indicated amounts of purified guinea pig liver TG2 (Sigma-Aldrich) in the presence or absence of 3 mM $CaCl_2$. This concentration of calcium was selected to assure maximal in vitro TG2 transamidation activity. For Ca^{2+}-free reactions, buffers were additionally supplemented with 2 mM EGTA. Reactions were incubated for up to 150 min at 37°C and terminated by the addition of 2× SDS-sample buffer (100 mM Tris HCl, pH 6.8, 4% (w/v) SDS, 20% (v/v) glycerol, 0.2% (w/v) bromophenol blue, 200 mM DTT) followed by heating for 5 min at 100°C. Reaction products were size-fractionated by SDS–PAGE using 10% polyacrylamide gels, transferred to nitrocellulose membranes, and processed for immunoblot analysis using the panel of anti-YB-1 antibodies described above. For in vitro TG2-mediated crosslinking assays using purified recombinant mouse N-HisYB1 as a substrate, a calcium/EGTA buffer system was used to precisely control free Ca^{2+} levels. The reaction buffer base consisted of 100 mM MOPS, pH 7.5, 0.2 mM PMSF, 1 mM DTT and protease inhibitor cocktail adjusted to various concentrations of free calcium using a 2 mM EGTA stock solution. Ca^{2+}/EGTA buffer formulations were determined using a free-access software program [Dweck et al., 2005]. Aliquots of N-HisYB1 were pre-warmed for 5 min at 37°C prior to adjusting the free calcium concentration with EGTA. Reaction mixtures containing varying amounts of purified guinea pig liver TG2 (0–1 mU/μl as noted in the text) were incubated for 60 min at 37°C and terminated by adding 2× SDS-sample buffer followed by heating at 100°C for 5 min. Reaction products were size-fractionated by SDS–PAGE on 10% polyacrylamide gels, transferred to nitrocellulose membranes, and processed for immunoblot analysis using anti-histidine or anti-YB-1 antibodies described above.

For in situ TG2-mediated crosslinking reactions [Oh et al., 2011], human pulmonary fibroblasts were incubated for 60 min with 1 mM biotinylated pentylamine substrate (EZ-link, Pierce, Rockford, IL) followed by an additional 60 min exposure to 1.5 mM hydrogen peroxide or vehicle. RIPA extracts were prepared as noted above followed by size-fractionation of TG2 reaction products by SDS–PAGE. Biotin-tagged fibroblast proteins were detected on blots using streptavidin-coupled horse radish peroxidase and standard chromagen-development chemistry (Invitrogen). To immunoprecipitate biotinylated YB-1 from the TG2 crosslinking reactions, 10 μg of anti N-terminal YB-1 polyclonal antibody (Sigma) was added to 200 μl of whole cell extract at a concentration of 1 mg/ml and allowed to incubate overnight at 4°C. Immune complexes were captured at 4°C by incubation for 90 min with a 50 μl aliquot of IgG-conjugated Dynabeads™ (M-280, anti-rabbit IgG, Invitrogen). The beads were placed on a magnetic stand and washed thrice in RIPA buffer. Immune complexes were eluted from the beads with 30 μl of 2× SDS sample buffer followed by heating at 100°C for 5 min and evaluated for the presence of biotinylated proteins by streptavidin-peroxidase immunoblot analysis. IgG-Dynabead control reactions also were performed using lysates in the absence of the immunoprecipitation capture antibody to assess non-specific adsorption of cellular proteins to the antibody-bead matrix.

TRANSGLUTAMINASE 2 siRNA KNOCK-DOWN AND ENZYME INHIBITION

To inhibit endogenous TG2 protein expression, a duplex siRNA sequence 5′AAGGGCGAACCACCTGAACAA-3′ was synthesized (Qiagen Sciences) and utilized in fibroblast-transfection studies to specifically ablate the coding sequence of human TG2 mRNA [Mann et al., 2006]. As a control for TG2-targeting specificity, cells also were transfected with a scrambled-sequence siRNA with no homology to any known mammalian gene (AllStars™ Negative control siRNA, Qiagen Sciences). For cell transfections, siRNA-liposomal complexes were pre-formed by incubating duplex siRNA with 3 μl RNAimax™ Lipofectamine reagent (Invitrogen) in 500 μl DMEM. After a 20 min incubation period, the mixture was added to pulmonary fibroblasts maintained at 40% confluent in six-well tissue-culture plates using antibiotic-free, DMEM/Ham's F12 growth medium (1:1) containing 10% hiFBS. Cells were harvested 72 h after transfection following exposure to either rhTGFβ1 (5 ng/ml) or vehicle during the last 24 h as noted in the text.

For TG2 enzyme inhibition studies, a stock solution of the competitive TG2 antagonist monodansylcadaverine (MDC; Sigma-Aldrich) was prepared fresh in DMSO and used for a 24 h dose–response study of YB-1 oligomer expression in human pulmonary fibroblasts maintained in complete growth medium. RIPA extracts were prepared from whole cells treated with either siRNA or MDC, size fractionated on denaturing SDS–PAGE, and processed for YB-1 immunoblot analysis as described above. The TG2-reactive site inhibitor cystamine (0.1–1 mM) also was used to inhibit transamidation in intact fibroblasts and RIPA extracts [Jeon et al., 2004] and diphenyleneiodonium chloride (DPI, Sigma-Aldrich) was used over a range of 2.5–30 μM to inhibit NADPH oxidase-mediated production of hydrogen peroxide in intact TGFβ1-activated fibroblasts, as previously described [Hecker et al., 2009].

RESULTS

RECOMBINANT MOUSE YB-1 IS A SUBSTRATE FOR TRANSGLUTAMINASE 2

Recent histologic analysis of post-transplant myocardial remodeling in accepted murine heart grafts using antibodies specific for the mRNA-binding CSD and C-terminal regions of YB-1 revealed the

presence of granular structures in both the peri-nuclear and intercalated disc regions [David et al., 2012]. This observation was consistent with the intrinsic ability of YB-1 to form large supramolecular structures [Selivanova et al., 2010] as well as cytosolic stress granules containing mRNAs that encode proteins required for cellular adaptation to metabolic stress [Nekrasov et al., 2003; Skabkin et al., 2004; Yang and Bloch, 2007; Chernov et al., 2008; Onishi et al., 2008]. In support of the idea that YB-1 oligomerization occurs in accepted heart grafts, immunoblot analysis of endomyocardial biopsies collected from heart transplant patients at various times during a 3-year post-operative period revealed YB-1 size variants migrating in the vicinity of the 150 kDa size marker (Fig. 1a). The relative resistance of YB-1 oligomers to dispersal during denaturing SDS–PAGE in the presence of reducing agents was suggestive of covalent protein crosslinking. In this regard, there are glutamine and lysine residues in the amino- and carboxyl-terminal regions, respectively, of YB-1 positioned within a larger secondary-structure context (QQPPA and RRRRPENPKP) previously associated with efficient transglutaminase 2 (TG2)-mediated transamidation [Csosz et al., 2008] and protein crosslinking (Fig. 1b). Recombinant 6XHIS-tagged mouse YB-1 (N-HisYB-1) was used as a substrate for purified porcine liver TG2 enzyme in reaction mixtures supplemented with an EGTA buffer to precisely control free calcium concentration [Dweck et al., 2005] in view of previous reports showing that TG2 transamidation activity is regulated by five low-affinity calcium-binding sites [Kiraly et al., 2009]. As shown in Figure 1c, 10–25 nM calcium was sufficient for the formation of high-molecular weight YB-1 oligomers in the presence of TG2. Consistent with its theoretical size of 35,924 Da, the recombinant form of mouse N-HisYB-1 purified from bacterial lysates migrates close to the p37 size marker. An additional major polypeptide band also was observed slightly below the p50 marker corresponding exactly to the observed mobility of SDS-denatured forms of native YB-1 expressed in mouse and human fibroblasts [Zhang et al., 2008; David et al., 2012]. N-HisYB-1 electrophoretic mobility was calcium-concentration dependent with p75–p125 variants clearly detected at 25 nM calcium. Between 100 and 500 nM free calcium, a broadly distributed group of less well resolved crosslinked products in excess of 250 kDa in size accumulated near the top of the 10% polyacrylamide running gel. Reaction products formed in the presence of either 1 or 100 μM calcium were not highly reactive with the anti-HIS mouse monoclonal antibody used to process the immunoblot shown in Figure 1c but detectable on the nitrocellulose transfer membrane after staining with Ponceau S red dye (data not shown). In addition, crosslinking reactions performed at supra-physiologic levels of calcium (1 and 100 μM) may have generated YB-1 oligomers that were too large to enter the SDS polyacrylamide gel. In contrast, YB-1 size heterogeneity in the vicinity of the p37–p50 size markers seemed biphasic with peak accumulation of multiple, distinct bands noted between 10 and 25 nM calcium as well as 1 μM calcium (Fig. 1c). No large-size variants were obtained in reactions performed in absence of TG2 consist with previous reports showing that YB-1 typically migrates in the 36–50 kDa size range on reducing SDS–PAGE [Zhang et al., 2008; David et al., 2012]. The complete absence of higher-order complexes larger than 36–50 kDa confirms that purified YB-1 does not spontaneously form polypeptide multimers in the absence of TG2 catalytic activity (Fig. 1c). The inability to detect YB-1 antibody-reactive bands in reaction mixtures lacking recombinant YB-1 eliminated spurious components in the liver TG2 enzyme preparation as a potential source for one or more of the 36–50 kDa bands detected in the presence of YB-1 substrate.

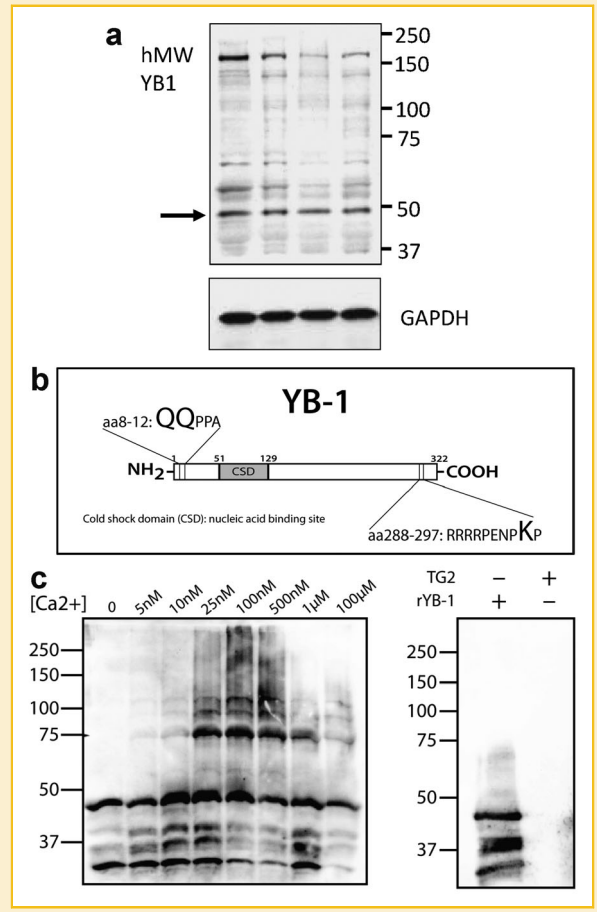

Figure 1. a: The *upper panel* depicts a YB-1 immunoblot prepared from endomyocardial biopsy-protein extracts collected from heart transplant patients at the 2, 10, 23, and 162 week post-transplant intervals (lanes from left to right). The prototypical YB-1 p50 band is denoted by the arrow and several higher molecular weight YB-1 bands (hMWYB1) proximal to the p150 marker are variably detected by a CSD-specific, anti-YB-1 antibody. The *lower panel* depicts GAPDH levels to show equivalent protein loadings in each lane of the immunoblot. b: Location of potential TG2-reactive amino acids in mammalian YB-1. Amino- and carboxyl-terminal regions of the YB-1 polypeptide contain respective glutamine and lysine residues that are potential substrates for TG2 transamidation. c: TG2-mediated YB-1 crosslinking is calcium dependent. The *left panel* depicts results obtained when purified recombinant, epitope-tagged N-HisYB-1 was used as a substrate for TG2 from guinea pig liver in reaction mixtures (60 min at 37°C) supplemented with an EGTA buffer to precisely control the free-calcium concentration. The immunoblot was processed using an anti-His antibody and indicates that formation of high-molecular weight YB-1 oligomers by TG2 was initiated between 10 and 25 nM free calcium. As shown in the *right panel*, immunoblots of reactions omitting TG2 enzyme did not reveal high-molecular weight YB-1 oligomers and omission of YB-1 substrate from reactions showed that oligomers were not the result of spurious contamination in the liver TG2 enzyme preparation.

TRANSGLUTAMINASE 2-CATALYZED YB-1 PROTEIN COMPLEXES ACCUMULATE DURING TGFβ1-DEPENDENT MYOFIBROBLAST DIFFERENTIATION

Formation of YB-1 protein complexes has not been examined in the regulatory context of myofibroblast differentiation and cardiopulmonary fibrosis. Early-passage, TGFβ1-activated human pulmonary myofibroblasts represent a potentially useful experimental model for examining the biochemical control of YB-1 oligomerization that avoids technical complications working with whole tissue specimens containing multiple cell types and histologic specializations. Myofibroblast differentiation induced by TGFβ1 was accompanied by enhanced expression of multiple YB-1 size variants with apparent molecular weights on SDS gels in the range of 75–250 kDa (Fig. 2a). Compared to the prominent p50 band, higher molecular weight YB-1 variants in TGFβ1-activated myofibroblasts generally were less abundant on immunoblots processed with any of the 4 anti-YB-1 antibodies used in our study. Accordingly, chemiluminescence image-capture times were varied over a period of 30–500 s to distinctly resolve the p50 and p75–250 weight regions on immunoblots that are depicted as separate digital-image components in Figure 2a. Importantly, formation of high-molecular weight YB-1 variants approximately 200–250 kDa in size was partly inhibited by 1 mM cystamine, a TG2 reactive-site inhibitor [Jeon et al., 2004], when administered to fibroblasts 60 min prior to a 16-h treatment with 5 ng/ml TGFβ1 (Fig. 2a). Further experimentation revealed that suppression of the smaller p100–125 YB-1 size variants required a higher amount of cystamine (2 mM) indicative of possible differential rates of YB-1 oligomer formation and/or stability [Willis and Strauch, data not shown]. Notably, high molecular weight forms of YB-1 appear to be transient components in TGFβ1-activated myofibroblasts. The ability to detect size variants in the range of p90–p250 was markedly reduced if cells were washed following an initial 7.5 h exposure to TGFβ1 and then incubated for an additional 7.5 h with fresh medium alone (Fig. 2b). However, large-size YB-1 variants were completely eliminated if the washed, TGFβ1-activated myofibroblasts were exposed to fresh medium supplemented with 5 U/ml thrombin for an additional 7.5 h (Fig. 2b). We previously reported that thrombin-mediated MEK1/Erk1,2 signaling dissociates YB-1 from a translation-silencing element in exon 3 of SMαA mRNA resulting in a rapid increase in SMαA protein synthesis [Zhang et al., 2005].

Suggesting that TGFβ1-associated TG2 transamidation in differentiated myofibroblasts may influence access of the N- and C-terminal segments of YB-1 oligomers to other proteins, we have observed that variants in the p100–p250 size range generally were more reactive with a commercial antibody specific for the N-terminal segment of YB-1 while variants migrating between the p37 and p75 were more reactive with a commercial antibody specific for amino acids proximal to the C-terminus [Willis and Strauch, unpublished observations]. Rabbit polyclonal antibodies developed by Kelm et al. [1999a] using a peptide antigen corresponding to amino acids 276–302 flanking the C-terminal end of the highly conserved YB-1 CSD (used to process the immunoblot depicted in Fig. 2b) as well as a peptide antigen encompassing amino acids 85–110 within the core of the CSD (used in Fig. 1a) both reacted with the full range of YB-1 size-variants observed in TGFβ1-activated myofibroblasts suggesting that these epitopes remain accessible following YB-1 oligomerization. Notably, the CSD and C-terminal regions are known to mediate interaction between YB-1 and single-strand nucleic acids and are thought to contribute to mRNA-translational control [Kohno et al., 2003; Nekrasov et al., 2003].

TRANSGLUTAMINASE 2 EXPRESSION AND BIOCHEMICAL CONTROL IN MYOFIBROBLASTS

TG2 has been implicated in the molecular regulation of tissue-stress response, fibrosis, and epithelial–mesenchymal transition that are cellular processes known to be associated with altered YB-1 subcellular compartmentalization [Mehta et al., 2010; Lin et al., 2011; Oh et al., 2011; Olsen et al., 2011]. Moreover, accumulation of peroxide in myofibroblasts due to elevated activity of NADPH oxidase [Hecker et al., 2009; Bondi et al., 2010] could injure mitochondria resulting in the release of intracellular calcium required for TG2 enzyme activation [Park et al., 2010; Gundemir et al., 2012]. Likewise, pro-fibrotic thrombin [Snead and Insel, 2012] releases intracellular calcium stores in myofibroblasts through its PAR-1 receptor [Sabri et al., 2002; Meoli and White, 2009] that may further augment TG2 crosslinking activity [Kiraly et al., 2009]. Thrombin also activates MEK1/Erk1,2 signaling in myofibroblasts that has been shown to dissociate YB-1 from SMαA mRNA, promote YB-1 nuclear translocation, and enhance both SMαA mRNA translation [Zhang et al., 2005] and actin-cytoskeleton assembly [Bogatkevich et al., 2003].

TG2 was constitutively expressed in human pulmonary fibroblasts as a 78 kDa protein that appeared to form protein dimers in response to TGFβ1 (Fig. 2c). Inclusion of hydrogen peroxide to simulate fibroblast peroxidative stress did not substantially alter TG2 expression or size distribution nor did it amplify the response to TGFβ1. Treatment with TGFβ1 alone or in combination with hydrogen peroxide caused a similar four- to fivefold increase in the level of TG2 dimer when normalized to GAPDH expression. To determine if native human YB-1 was an authentic substrate for TG2 transamidation, pulmonary fibroblasts were exposed to a membrane-permeable, biotinylated primary amine that serves as a surrogate lysine substrate for the TG2 transamidation reaction [Oh et al., 2011]. Endogenous TG2 activity in fibroblasts was sufficient to crosslink the biotinylated pentylamine (BP) substrate to accessible glutamine residues in a protein migrating near the 50 kDa size marker that was identified as YB-1 based on immunoprecipitation from fibroblast extracts using a YB-1 antibody (Fig. 2d). TGFβ1 was not used in this experiment to limit YB-1 oligomerization that could prevent access of BP substrate to reactive glutamines in the N-terminus of YB-1. Exogenous ROS provided in the form of hydrogen peroxide was not required for TG2-mediated biotinylation of p50 YB-1 nor did it enhance the specific immunoprecipitation of biotin-YB-1 suggesting that the TG2 enzyme is active in fibroblasts under these particular experimental conditions.

To account for possible low permeability of the BP substrate and/or poor equilibrium with the YB-1 pool that could limit detection of endogenous TG2 reaction products in intact pulmonary fibroblasts, we performed a second crosslinking reaction using exogenous TG2 enzyme purified from guinea pig liver to crosslink native YB-1 in fibroblast lysates prepared using RIPA extraction buffer. Increasing amounts of liver TG2 were added to RIPA lysates under a condition of calcium excess (3 mM) to assure high-level TG2 enzymatic activity over the 150 min reaction performed at 37°C [Kiraly et al., 2009; Dai

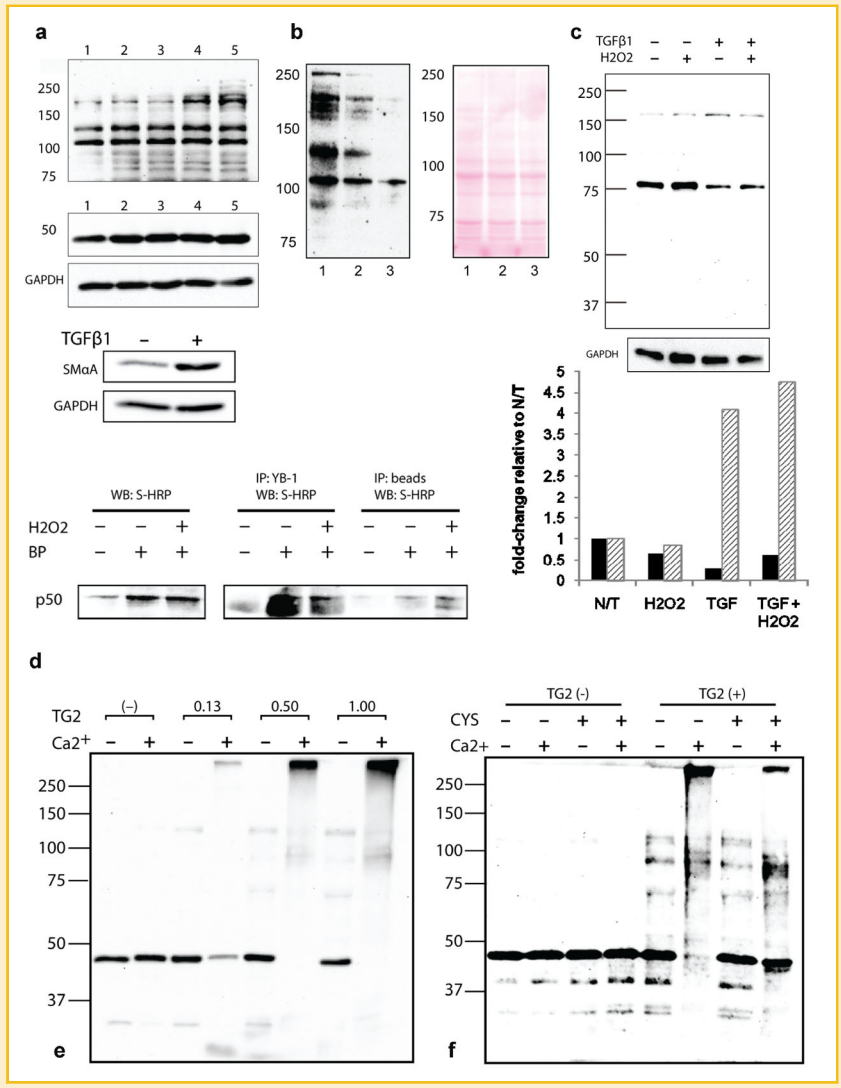

Figure 2. a: *Upper panels*: formation of p150–p250 YB-1 oligomers in TGFβ1-activated myofibroblasts was attenuated by cystamine inhibition of TG2 enzyme activity. Lane 1: no treatments; lane 2: cystamine alone (1 mM); lane 3: TGFβ1 + cystamine (1 mM); lane 4: TGFβ1 + cystamine (0.1 mM); lane 5: TGFβ1 alone. Cells were treated with vehicle or cystamine for 60 min prior to adding TGFβ1 (5 ng/ml) for an additional 16 h. Whole cell lysates were prepared using RIPA buffer as noted in the methods. The p50 and p75–p250 regions of the immunoblot were processed at the same time using a N-terminal-specific anti-YB-1 antibody but are presented as separate images and were captured using two different exposure settings during development of the chemiluminescence signal. *Lower panel*: SMαA expression in quiescent human pulmonary fibroblasts maintained in low-serum (0.5%) medium typically increases several fold in response to TGFβ1 treatment (5 ng/ml; 24 h). b: YB-1 oligomers in TGFβ1-actived myofibroblasts are transient and rapidly depleted by thrombin. Monolayers of human pulmonary fibroblasts were treated with TGFβ1 (5 ng/ml) for 15 h (lane 1) or washed after 7.5 h and transferred to medium without TGFβ1 (lane 2) or medium containing thrombin (lane 3) for another 7.5 h before preparing cytosolic extracts. Thrombin treatment (5 U/ml) resulted in dispersion of several high molecular weight oligomers upward of p100 kDa in size. A depiction of the transfer membrane stained with Ponceau S red is shown on the right indicating equivalent protein loadings of the 3 lysate samples. c: TG2 protein migrated as a single 75 kDa polypeptide on SDS–PAGE that appeared to form dimers when human pulmonary fibroblasts were exposed to TGFβ1 or a combination of TGFβ1 and hydrogen peroxide (*upper panel*). Fibroblasts were treated with vehicle or TGFβ1 (5 ng/ml) for 16 h followed by vehicle or peroxide (1.5 mM) 1 h prior to harvest. For the graph shown in the *lower panel*, the relative amount of TG2 monomer (solid bar) and dimer (hatched bar) was normalized to GAPDH expression. Baseline expression in the untreated control preparation (N/T) was set to 1 and treatment outcomes were recorded in terms of fold-change relative to control. d: YB-1 is a target for TG2 crosslinking in human pulmonary fibroblasts. Fibroblasts were pre-treated with a biotin-pentylamine TG2 substrate (BP, 1 mM, 60 min) followed by vehicle or peroxide (1.5 mM) for an additional hour prior to cell harvest. Treatment with BP alone or the combination of BP and peroxide resulted in detection of a biotin-tagged p50 polypeptide (*left panel*) that was identified as YB-1 by immunoprecipitation (IP) from RIPA lysates using an anti-YB-1 polyclonal antibody followed by streptavidin-HRP (S-HRP) western blot (WB) analysis (*right panel*). Minor, non-specific association of spurious biotinylated p50 protein with the IgG-conjugated beads was noted in bead-only IP control preparations but abundant biotinylated YB-1 was captured using these beads in combination with an anti-YB-1 antibody. e: Aliquots of RIPA lysates prepared from pulmonary fibroblasts were combined with purified liver TG2 (0.13–1.00 mU/μl) in the presence of a transamidation-reaction buffer containing 3 mM calcium. Within a 150 min reaction period, TG2 concentration-dependent crosslinking of p50 YB-1 was detected by immunoblot analysis with notable accumulation of calcium-dependent, high-molecular weight products in excess of 250 kDa. f: TG2-dependent crosslinking of YB-1 in fibroblast RIPA lysates was suppressed by the cystamine TG2 active-site inhibitor. Cystamine (1 mM) partially prevented formation of high-molecular weight YB-1 by TG2 (0.50 mU/μl) in the presence of calcium while enhancing the level of YB-1 variants in the vicinity of the 100 kDa size marker.

et al., 2011; Gundemir et al., 2012]. TG2 efficiently catalyzed the formation of a large YB-1 oligomeric complex with an apparent mass greater than 250 kDa (p250+) but only in lysates supplemented with excess calcium (Fig. 2e). Increasing the concentration of TG2 in reaction mixtures resulted in the incorporation of all available p50 YB-1 into the high molecular weight complex. Inclusion of cystamine, a TG2 transamidation reactive-site inhibitor [Jeon et al., 2004; Mishra and Murphy, 2006], reduced accumulation of the p250+ YB-1 oligomer in crosslinking reactions while preserving p50 YB-1 and enhancing the presence of the 100 kDa variant (Fig. 2f). The p100 size variant may correspond to a conformational intermediate (possibly a dimer) derived from rapid transamidation of p50 YB-1 monomer but unable to transition into p250+ oligomer before TG2 arrest by the cystamine transamidation inhibitor.

TGFβ1 has been shown to stimulate production of hydrogen peroxide, an important mediator of myofibroblast differentiation and pulmonary fibrosis [Hecker et al., 2009]. Moreover, reactive oxygen intermediates reportedly augment both NFκB-mediated TG2 gene transcription and TG2 transamidation activity [Ientile et al., 2007]. NADPH oxidase 4 (*NOX4*) has been identified as a TGFβ1-responsive enzyme potentially responsible for ROS accumulation in pulmonary myofibroblasts. We therefore examined the effect of the general NADPH oxidase inhibitor, diphenyleneiodonium chloride (DPI), that was shown to reduce collagen secretion and accumulation of SMαA-positive myofibroblasts in a mouse model of bleomycin-induced pulmonary fibrosis [O'Donnell et al., 1993; Hecker et al., 2009]. As shown in the upper panel of Figure 3a, DPI effectively reduced accumulation of the same types of YB-1 size variants expressed in TGFβ1-activated human pulmonary myofibroblasts that were shown to be a result of TG2-mediated transamidation. While the level of p50 YB-1 was not significantly altered by DPI treatment, expression of both p100 and p125 variants was completely diminished by 2.5 μM DPI concomitant with the appearance of a novel YB-1 size variant somewhat larger than p125 (p125+) that also became depleted but more gradually over the range of 2.5–30 μM DPI. Notably, depletion of the novel p125+ variant occurred in parallel with a graded reduction in SMαA protein expression in DPI-treated pulmonary myofibroblasts (lower panel, Fig. 3a). We additionally examined the effect of the TG2 inhibitor monodansylcadaverine (MDC) on YB-1 oligomerization. MDC is a reversible competitive antagonist to TG2 enzyme activity that competes with endogenous lysine substrates for the transamidation reaction [Badarau et al., 2013]. MDC suppressed expression of the p250+ YB-1 variant and, to a lesser extent, the p125 variant in a concentration-dependent manner over a 24 h exposure period (Fig. 3b). Suppression of the p250+ YB-1 complex, in particular, occurred in parallel to MDC-dependent reduction of SMαA protein expression in MDC-treated myofibroblasts (Fig. 3b). Additionally, we observed that TG2-specific, short-interfering RNA (siRNA) effectively suppressed expression of TG2 protein as well as accumulation of the p125 YB-1 variant in a concentration dependent manner in human pulmonary fibroblasts (Fig. 4a). This finding suggested that transamidation enzymatic activity associated with YB-1 oligomerization was largely a function of TG2 isozyme availability as opposed to some other member of the transglutaminase family that might be co-expressed in pulmonary fibroblasts. Recent studies showed that siRNA knockdown of TG2 protein expression in human pulmonary fibroblasts resulted in impaired TGFβ1-dependent adhesion and contraction on collagen-gel substrates [Olsen et al., 2011]. In this regard, TG2-specific siRNA partially reduced the level of unpolymerized SMαA actin detected in supernatants prepared from the cytosol fraction of either quiescent human pulmonary fibroblasts or TGFβ1-activated myofibroblasts (Fig. 4b).

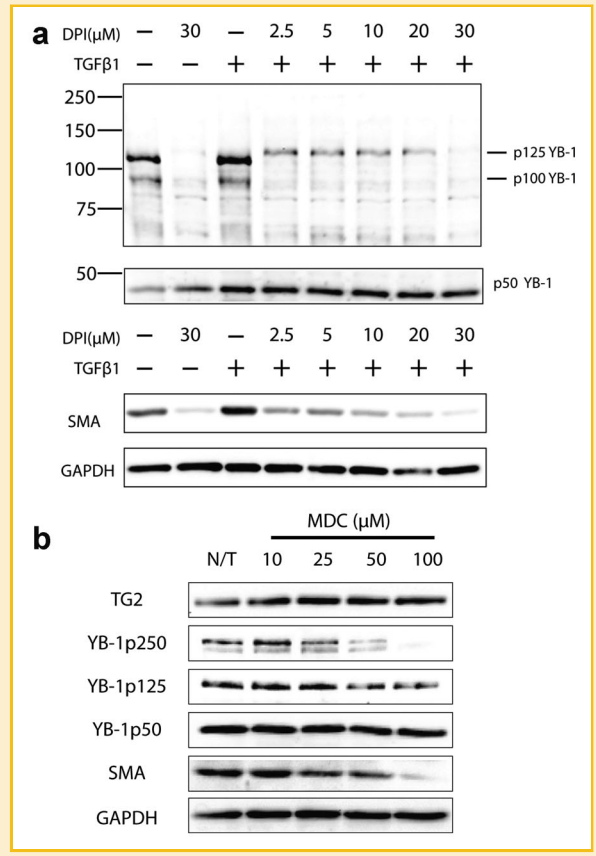

Figure 3. a: Diphenyleneiodonium (DPI) reduced accumulation of oligomeric forms of YB-1 expressed in TGFβ1-activated human pulmonary myofibroblasts. The *top panels* show that expression of high molecular weight variants of YB-1 were induced by TGFβ1 but depleted when cells were exposed to various amounts of DPI (2.5–30 μM) for 24.5 h either in the presence or absence of TGFβ1 (5 ng/ml). Cells were exposed to DPI 30 min prior to addition of TGFβ1 and then processed using RIPA lysis buffer. Expression of the p100 YB-1 variant was completely suppressed at low dosages of DPI while a slightly larger variant (p125) initially was upwardly size-shifted at 2.5 μM DPI and then depleted in an inhibitor concentration-dependent manner. The *bottom panels* show that the observed depletion of YB-1 p125 variant occurred in parallel to DPI-induced reduction in SMαA protein expression. b: YB-1 oligomers in SMαA-positive human pulmonary myofibroblasts were selectively suppressed by the TG2 inhibitor monodansylcadaverine (MDC). Cells were exposed to various amounts of MDC (10–100 μM) for 24 h and processed using RIPA lysis buffer. p250 YB-1 and, to a lesser extent, p125 were suppressed by MDC in a concentration-dependent manner. Suppression of these size variants by MDC was accompanied by a reduction in SMαA protein expression.

YB-1 SIZE-VARIANTS BIND A TRANSLATIONAL SILENCING ELEMENT IN SMαA mRNA

Exon 3 in SMαA mRNA contains a high-affinity binding site for YB-1 that is required for mRNA translational repression in fibroblasts and

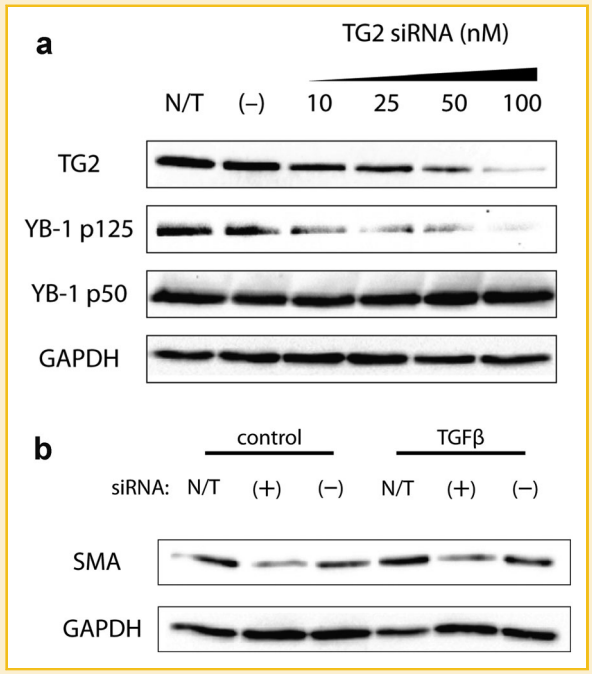

Figure 4. a: Suppression of p125 YB-1 oligomer by siRNA-mediated inhibition of TG2 protein expression. Human pulmonary myofibroblasts were transfected with 100 nM of either scrambled/negative control siRNA (–) or various amounts of TG2-specific siRNA (10–100 nM). Whole cell lysates were prepared using RIPA buffer. siRNA reduced expression of TG2 as well as the YB-1 p125 oligomer in a siRNA-concentration dependent manner but slightly elevated expression of p50 YB-1. b: TG2 siRNA partially suppressed expression of unpolymerized SMαA protein in supernatants prepared from the cytosolic fraction of human pulmonary fibroblasts (control) and myofibroblasts (TGFβ). Cells were transfected with 10 nM TG2 siRNA (+) or scrambled siRNA (–) for 48 h prior to treatment with either vehicle (control) or TGFβ1 (TGFβ) for an additional 24 h. N/T denotes cells that did not receive siRNA or transfection reagents.

smooth muscle cells [Kelm et al., 1999b; Zhang et al., 2005]. Some YB-1 size variants present in TGFβ1-activated pulmonary myofibroblasts were capable of enhanced binding to oligonucleotide probes derived from various regions of human SMαA mRNA. Protein retained on RNA-beads following incubation with extracts prepared from pulmonary fibroblasts in the presence or absence of TGFβ1 was processed for immunoblot analysis using an antibody specific for the YB-1 CSD that mediates mRNA binding [antibody 85–110, Kelm et al., 1999a,b]. As depicted in Figure 5, an oligoribonucleotide encompassing the exon-3 mRNA-binding site for YB-1 (CERNA) captured, in a TGFβ1-dependent manner, several YB-1 size variants migrating on SDS–PAGE immunoblots in the vicinity of the p50–p100 size markers. A second RNA that contained a similar exon 3-like sequence motif but derived from the 3′-untranslated region (3′UTR) of SMαA mRNA showed enhanced binding to the p125 YB-1 size variant in TGFβ1-activated myofibroblasts but exhibited rather weak interaction with p50 that was unaffected by TGFβ1. In contrast, two other oligoribonucleotides (CSD1 and CSD4) derived from exons in SMαA mRNA that were partially homologous to RNA sequences with known binding affinity for YB-1 and other cold-shock domain proteins [Coles et al., 2004] interacted with some of the YB-1 size variants but binding in this instance was not enhanced by TGFβ1. Data presented in Figure 5 suggests that several YB-1 size variants that accumulate in myofibroblasts were able to bind a known translational silencing element in SMαA mRNA that is under control of TGFβ1 and thrombin signaling.

YB-1 oligomers may perform tasks in injury-activated myofibroblasts associated with stabilizing, sequestering, or transporting mRNAs encoding specialized proteins required for cell-type specific functions or basic survival during periods of metabolic stress [Nekrasov et al., 2003; Skabkin et al., 2004; Yang and Bloch, 2007; Strauch and Hariharan, 2013]. Physical interaction of p50 YB-1 with mRNAs that encode proteins serving these needs might facilitate TG2 crosslinking possibly by positioning glutamine and lysine substrate moieties within the transamidation active site. To assess the general effect of mRNA on TG2-mediated YB-1 crosslinking, a 30-nt oligoribonucleotide fragment encompassing the YB-1-binding site in exon-3 of SMαA mRNA was incubated with recombinant N-HisYB-1 prior to addition of liver TG2. As shown in Figure 6a, YB-1 in the absence of TG2 and RNA migrated as a single p50 band. Upon addition of TG2 in the presence of 3 mM calcium to maximize transamidation activity, apparent YB-1-size isomerization was observed producing a poly-dispersed array of poorly resolved bands around p50 in size plus protein complexes greater than 250 kDa in size. In the presence of RNA, conversion of p50 YB-1 into higher order complexes was more robust than reactions containing TG2 alone on a per-unit N-HisYB-1 protein-mass basis (Fig. 6a). To examine the ability of native YB-1 to bind mRNA in relation to the level of SMαA protein synthesis in human fibroblasts, we utilized exon 3 mRNA-affinity beads to capture YB-1 from whole cells extracts prepared from TGFβ1-activated human pulmonary myofibroblasts as well as several early-passage preparations of human pulmonary-artery adventitial fibroblasts (PAAFs) that were classified as having either low- or high-level constitutive expression of SMαA protein. As shown in the immunoblot presented in Figure 6b that was processed using an antibody specific for the N-terminal region of YB-1, SMαA exon-3 mRNA affinity beads captured p50 YB-1 plus another variant around 37 kDa in size from all the extracts. Of note, several additional antibody-reactive bands corresponding approximately to the p100 and p125 forms of YB-1 described earlier in this report were variably enriched in extracts prepared from TGFβ1-activated pulmonary myofibroblasts (HPFBs) and more robustly in PAAFs exhibiting high-output production of SMαA polypeptide (UP89, UP72, UP88). These observations indicate that the exon-3 element in SMαA mRNA can capture native, YB-1-containing protein complexes and that this binding activity appears to be selectively enriched in YB-1 oligomers present in fibroblasts capable of high-output SMαA protein synthesis (Fig. 6c).

TRANSGLUTAMINASE 2 MEDIATES BOTH THE FORMATION AND DISPERSION OF YB-1 OLIGOMERS

TG2 has intrinsic isopeptidase activity capable of hydrolyzing protein crosslinks caused by transamidation. The isopeptidase activity results in the deamidation of constituent glutamine residues to glutamic acid especially in the presence of high concentration of TG2 enzyme [Stamnaes et al., 2008]. Reverse YB-1 crosslinking due to deamidation could explain the apparent dispersal of high molecular weight forms

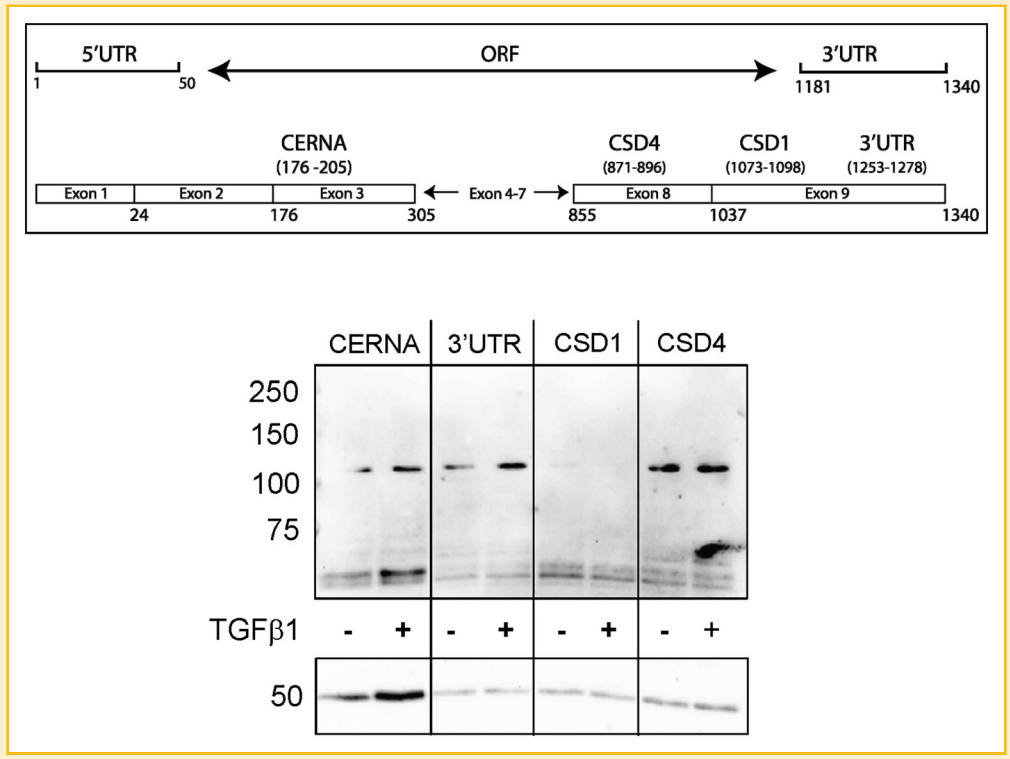

Figure 5. YB-1 p50 and p100 variants bound oligonucleotide probes derived from various regions of human SMαA mRNA. The *upper panel* shows diagram depicting the origins of the four biotinylated SMαA mRNA probes used for the RNA pull-down and immunoblot analysis depicted in *lower panel*. The p100 form of YB-1 present in RIPA lysates prepared from human pulmonary fibroblasts bound to the CERNA and 3′UTR probes in a TGFβ1-dependent manner while binding to other exonic sequences in SMαA mRNA with potential affinity for CSD proteins (CSD1, CSD4; refer to the *upper panel*) was not enhanced by TGFβ1. Also, p50 binding to the CERNA sequence, but not the other probes, increased in response to TGFβ1 treatment.

of YB-1 observed after exposure of TGFβ1-activated myofibroblasts to thrombin as shown in Figure 2. To examine if YB-1 crosslinks can be reversed experimentally, mixtures of liver TG2 and N-His-YB-1 were evaluated by SDS–PAGE immunoblot at various times over a 150-min reaction period (Fig. 7). To assure adequate accumulation of high molecular weight YB-1 as substrate and to enhance the efficiency of TG2 isopeptidase activity, calcium level was held constant at 3 mM and a second aliquot of enzyme was added approximately midway in the reaction period to increase TG2 concentration about eightfold (Fig. 7a). In reactions initiated with 0.125 mU/μl of TG2, YB-1 was resolved during the first 30-min interval as a series of closely migrating bands in the range of 37–50 kDa followed 15 min later by a broad accumulation of poorly resolved high-molecular material distributed between the 100 and 250 kDa size markers (45 min, Fig. 7b). Increasing the concentration of TG2 to 1.0 mU/μl at the 75-min interval further shifted distribution of YB-1 size variants toward the upper end of the SDS gel by the 90 min time point but also resulted in re-appearance of p50 over the next 30-min interval (120 min, Fig. 7b). Re-appearance of p50 was transient and its loss during the final 30 min of the reaction following replenishment of TG2 enzyme most likely was due to concurrent transamidation and re-incorporation into high molecular weight YB-1. Significantly less crosslinked product formed over the course of the full 150-min reaction was able to enter the 5% stacking gel compared to the earlier time points (150 min, Fig. 7b) although epitope masking within large-size YB-1 complexes also could explain reduced antibody reactivity with these particular samples. To optimize detection of p50 YB-1 monomer that would signify oligomer dispersion, the immunoblots depicted in Figure 7 were processed using an antibody specific for the C-terminal region of YB-1 that is highly reactivity with monomeric forms of YB-1.

Early in the crosslinking reaction, monomeric YB-1 may form a hypothetical calcium/TG2-dependent transition state that is susceptible to nucleophilic attack by a C-terminal lysine residue in a second YB-1 molecule to form an isopeptide linkage and higher-order YB-1 oligomer (Fig. 7c). However, in the absence of an amine substrate, other investigators have shown that water can serve as the attacking nucleophile within the TG2 enzyme-substrate complex (Fig. 7c) resulting in glutamine deamidation rather than transamidation [Stamnaes et al., 2008]. Similarly, dispersal of YB-1 oligomers to monomers via TG2 isopeptidase activity may be accomplished under solvent conditions that transiently expose shielded isopeptide bonds within the oligomer to nucleophilic attack. Consistent with this idea, partial depletion of the p250+ YB-1 oligomer pool with concurrent accumulation of variants in the p50–p100 size range was observed within 15 min after addition of the second aliquot of TG2 enzyme in reactions where the ionic strength was increased using NaCl (Fig. 7d). Similarly, oligomer dispersal was enhanced if the reaction was

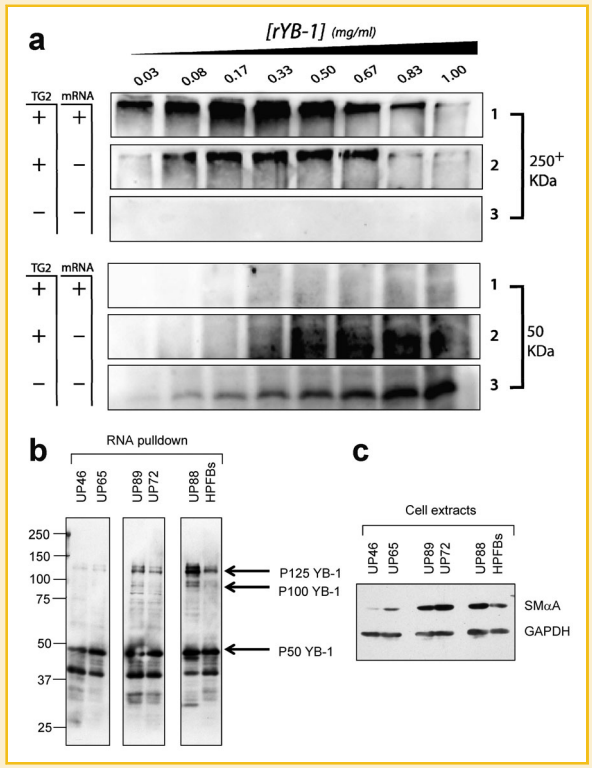

Figure 6. An exon 3 translational silencing element in SMαA mRNA enhanced TG2-mediated YB-1 crosslinking and captured native YB-1 oligomers in SMαA-positive myofibroblasts. a: Selected portions (*rows 1–3*) of SDS–PAGE immunoblots processed with an anti-His antibody are presented that depict optimized chemiluminescence detection of YB-1 electrophoretic variants migrating in either the 50 or 250+ kDa regions following a 30 min crosslinking reaction performed at 37°C using a fixed amount of TG2 enzyme (0.3 mU/μl) in the presence of excess calcium (3 mM) plus varying amounts of recombinant N-HisYB-1 (rYB-1) with or without the exon 3 CERNA mRNA oligonucleotide (0.5 μM). In the absence of TG2 and mRNA, recombinant N-HisYB-1 migrated as a single p50 band (*row 3* samples). Addition of TG2 alone caused apparent size-isomerization of p50 YB-1 and formation of protein complexes in excess of 250 kDa (*row 2* samples). Inclusion of both TG2 and the exon 3 fragment of SMαA mRNA resulted in the complete conversion of YB-1 p50 into a high-molecular weight complex (*row 1* samples). Native forms of oligomeric YB-1 demonstrated mRNA-binding activity (panel b) and appear specifically enriched in nuclear-protein extracts prepared from fibroblasts exhibiting high-level SMαA expression (panel c). Protein captured by mRNA-affinity beads from nuclear extracts prepared from two human adventitial fibroblast preparations with low baseline expression of SMαA (UP46 and UP65) was enriched for p50 plus a second form of YB-1 that migrated close to the 37 kDa size marker. In contrast, several additional bands proximal to the 100 kDa size marker were detected in nuclear extracts prepared from adventitial fibroblasts that highly express SMαA protein (UP89, UP72, UP88) as well as TGFβ1-activated human pulmonary myofibroblasts (HPFBs). RIPA whole cell lysates were prepared from fibroblasts for assessment of SMαA and GAPDH expression as shown in panel c.

supplemented with single-stranded DNA (Fig. 7e). Similar to the effect of increasing the ionic strength with salt, interaction of YB-1 oligomer with the sugar-phosphate backbone of the DNA oligonucleotide may alter the isopeptide bond microenvironment to facilitate deamidation. Recovery of p50–p100 size-class variants in the NaCl- or nucleic acid-treated reaction mixtures (Fig. 7d,e) was higher at the 90 min observation point compared to reactions that received no solvent adjustments (Fig. 7b). Specific accumulation of the presumptive p50 monomer, however, was somewhat delayed in the nucleic acid-treated reactions requiring an additional 30 or 60 min compared to water and NaCl, respectively.

DISCUSSION

YB-1 is believed to repress SMαA promoter activity in quiescent stromal fibroblasts by binding the reverse strand of an essential MCAT/THR *trans*-activation element that is known to undergo chromatin-conformational changes in response to TGFβ1 signaling [Becker et al., 2000]. During TGFβ1-mediated myofibroblast differentiation, YB-1 dissociates from the MCAT/THR element and the SMαA promoter is re-folded into duplex DNA upon binding of the Smad 2/3, Sp1/3, and serum response factor (SRF) transcriptional activators to their cognate binding sites [Eliseeva et al., 2011; Strauch and Hariharan, 2013]. Smad protein-facilitated displacement of YB-1 from the MCAT/THR within the TGFβ1-activated SMαA promoter appears to be coupled to nuclear export of ribonucleoprotein complexes consisting of YB-1 oligomers and newly transcribed SMαA mRNA [Zhang et al., 2005]. Although the functional significance of this finding remains unclear, tissue injury-activated formation of nuclear YB-1 ribonucleoprotein complexes in myofibroblasts may facilitate delivery of SMαA mRNA to polyribosomes for preferential actin G-monomer biosynthesis that allows fast polymerization of F-actin filaments needed for granulation tissue contraction and wound closure. Post-transcriptional mechanisms that modify mRNA stability and/or translational efficiency provide rapid and flexible control of gene expression that may be particularly important in coordinating not only the initiation but, more critically, prompt resolution of myofibroblast differentiation during wound-healing [Anderson, 2010]. We speculate that the fibrogenic agonist thrombin assists TGFβ1-activated transcription during wound healing by functioning as a post-transcriptional modifier through its ability to activate Erk1/2 kinases that stimulate displacement of YB-1 from the exon-3 translation-silencing element in SMαA mRNA [Zhang et al., 2005]. This YB-1-binding site is proximal to the 5′ AUG translation-start codon based on several thermodynamically favorable stem-loop models constructed from the full-length SMαA mRNA sequence and may help regulate ribosome access to the 5′ cap structure [Willis and Strauch, unpublished data]. Displacement of YB-1 from the stockpile of nascent myofibroblast mRNAs including transcripts encoding SMαA and type I collagen subunits [Hanssen et al., 2011] may relieve translational repression and permit rapid accumulation of specialized proteins needed to mount an efficient wound healing response.

Using both native and recombinant YB-1 as substrates, we have shown that TG2 catalyzes the formation of YB-1 oligomers that retain selective affinity for certain CSD protein-binding sequences in SMαA mRNA. YB-1 protein dimers may nucleate calcium-dependent assembly of higher-order multimers that while seemingly resistant to heat- and SDS-denaturation nonetheless might be dissociable by deamidation mediated by the intrinsic isopeptidase activity of TG2 [Stamnaes et al., 2008]. Others have shown that multimers of YB-1 reportedly influence globin mRNA translational efficiency in

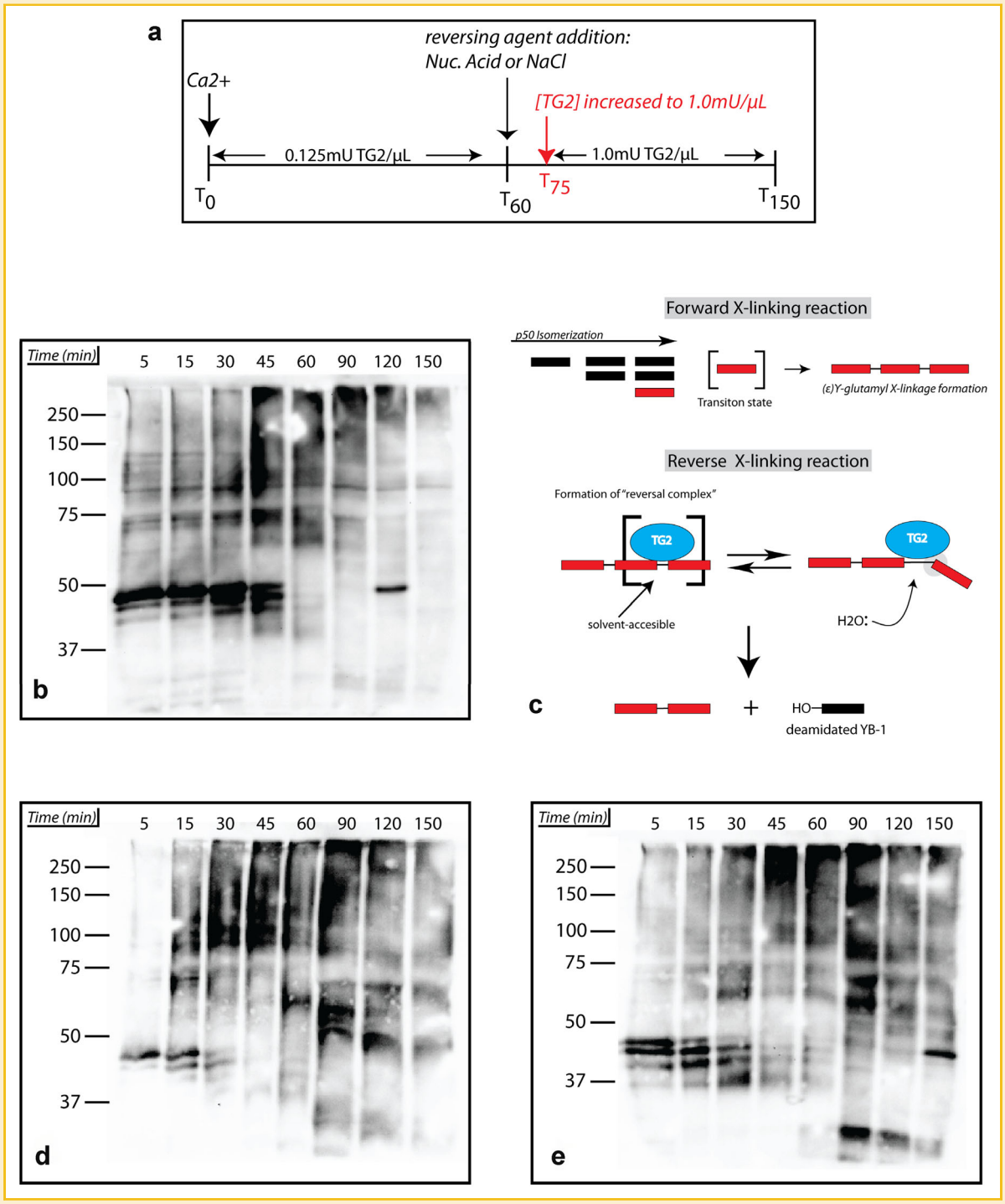

Figure 7. TG2-mediated crosslinking of YB-1 is partially reversible. The experimental scheme is presented in panel (a). Purified recombinant N-HisYB-1 and liver TG2 (0.125 mU/μl) were combined in a calcium-supplemented (3 mM) reaction buffer. Aliquots for SDS–PAGE were removed at various times during the 150 min reaction period. At the 60 min time-point, the reaction was supplemented with a nucleophile (500 mM NaCl or DNA) followed 15 min later with a second aliquot of TG2 to increase the final enzyme concentration to 1.0 mU/μl for the duration of the reaction. Panel b depicts a crosslinking reaction where TG2 was increased at the 75 min time-point resulting in the transient accumulation of p50 YB-1 monomer at the 120 min time-point. Panel c depicts the hypothetical models for forward and reverse TG2-mediated crosslinking. Panel d shows that addition of NaCl (500 mM) at the 60 min interval prior to adding additional TG2 enzyme to the reaction slightly enhanced the rate of crosslink reversal relative to that seen in (b). Size variants between 50 and 75 kDa were first detected in the presence of NaCl at the 90 min interval. In contrast, panel e shows that addition of DNA at 60 min (1:1, mole ratio of DNA/YB1) delayed appearance of p50 YB-1 until the 150 min interval.

reticulocyte lysates [Nekrasov et al., 2003; Skabkin et al., 2004] and TG2 transamidation is well known as an extracellular enzymatic reaction required for matrix-protein crosslinking, fibrosis, and cell adhesion [Chou et al., 2011]. Nearly two decades ago, Rifkin and co-workers showed that TG2 transamidation was linked to activation of latent TGFβ1 in endothelial cells [Kojima et al., 1993]. More recently, expression of TG2 in fibroblasts was shown to increase TGFβ1 bioavailability [Telci et al., 2009] and that mice lacking a functional TG2 gene were protected from renal and pulmonary fibrosis [Gundemir et al., 2012]. In age-associated syndromes such as vascular hypertension, excessive peri-vascular deposition of active TG2 reduces proteolytic clearance of crosslinked matrix proteins resulting in adventitial fibrosis and loss of arterial compliance [Santhanam et al., 2010]. Our study extends these observations and further indicates that transglutaminase 2 may perform important physiologic tasks inside the cell. TG2-mediated transamidation may adjust the proteome to the particular needs of wound-healing biochemistry by deploying YB-1 oligomers that capture and stabilize mRNAs encoding specialized proteins needed to repair damaged tissue. Others have shown that intracellular TG2 helps maintain the functional integrity of mitochondrial electron transport and augments signaling pathways associated with epithelial–mesenchymal transition needed for repair of damaged epithelial cells and their associated basement membrane [Mehta et al., 2010; Lin et al., 2011; Oh et al., 2011; Olsen et al., 2011; Gundemir et al., 2012]. In the nucleus, TG2 crosslinks and governs the action of transcriptional regulatory proteins including Sp1, hypoxia-inducible factor, retinoblastoma protein, and the E2F1 cell-cycle regulatory protein that could regulate cell proliferation and angiogenesis in healing wounds [Kuo et al., 2011].

YB-1 complexes have not previously been described in the context of myofibroblast differentiation prompting us to consider regulatory signals that could govern YB-1 oligomerization in specific response to biochemical conditions within the healing wound. TGFβ1 activates NADPH oxidase-mediated production of reactive oxygen intermediates and the associated oxidative stress responses that transpire in both the heart [Kuroda et al., 2010] and lung [Hecker et al., 2009] have been linked to fibrosis and dysfunctional cardiopulmonary remodeling. In addition, thrombin amplifies the action of TGFβ1 in myofibroblasts by releasing intracellular calcium via activation of PAR1 receptor-coupled G proteins [Snead and Insel, 2012]. Thrombin-dependent calcium release could promote F-actin polymerization and actomyosin contractility downstream from the initial burst of SMαA gene transcription mediated by the TGFβ1-dependent Smad3 *trans*-activator protein [Howell et al., 2002; Bogatkevich et al., 2003, 2005; Zhang et al., 2005; Strauch and Hariharan, 2013]. Importantly, TG2 transamidation activity is augmented by both intracellular calcium and reactive oxygen intermediates that are the most likely agonists for YB-1 oligomerization in TGFβ1-activated myofibroblasts.

Although the complete consensus-substrate sequence for TG2 transamidation has not yet emerged, there is a preference for protein targets that are classified as intrinsically disordered and have glutamine and lysine residues situated adjacent to proline [Csosz et al., 2008]. TG2-reactive glutamine and lysine substrates also tend to reside within N- and C-terminal regions, respectively. While the lysine-substrate preference of TG2 is largely dependent on the tertiary structure of target proteins [Murthy et al., 2009], a peptide consensus sequence for the arrangement of glutamine substrates has been reported. Using phage-display selection methods Keresztessy and colleagues formulated a general consensus motif for TG2 glutamine substrates as pQx(P, T, S)l, where x is any amino acid, p is a polar amino acid, and l corresponds to an aliphatic amino acid [Keresztessy et al., 2006]. Examination of the YB-1 primary sequence revealed the presence of a potential glutamine substrate in the N-terminus. We speculate that YB-1 crosslinking occurs when the N-terminal glutamine substrate forms an acyl-enzyme intermediary complex within the TG2 active site. The C-terminal lysine substrate provided by a second YB-1 monomer could complete formation of a γ-glutamyl isopeptide linkage via nucleophilic attack on the glutamine-TG2 acyl enzyme complex. C-terminal regions of the YB-1 polypeptide chain appear to be partially masked in high-molecular weight oligomers in view of their observed lower avidity for an antibody generated against C-terminal epitopes. On the other hand, YB-1 variants distributed within the 37–100 kDa size range reacted quite well with the C-terminal-specific antibody. Conversely, YB-1 antibodies generated against either N-terminal or CSD epitopes showed relatively high avidity for the large YB-1 oligomers. While the mechanistic significance of C-terminal epitope masking in extensively oligomerized YB-1 currently is not known, this region of YB-1 contains four alternating clusters of basic and acidic amino acids forming a charged zipper that recognizes specific RNA stem-loop structures and provides a docking site for other proteins [Kohno et al., 2003; Nekrasov et al., 2003; Eliseeva et al., 2011]. As shown in this report, YB-1 crosslinking by TG2 does not impair protein molecular structure required for post-oligomerization acquisition of mRNA payload. Indeed, native YB-1 oligomers that naturally form within SMαA-positive myofibroblasts possess intrinsic mRNA-binding activity and can be isolated from lysates using RNA affinity-binding methods. Moreover, synthetic oligomer formation in vitro was more favorable when TG2 transamidation reactions were supplemented with sequence segments of SMαA mRNA.

TG2 transamidation reportedly is reciprocally regulated by GTP and calcium levels [Begg et al., 2006; Kiraly et al., 2009; Stamnaes et al., 2010; Gundemir et al., 2012]. In the realm of pathophysiology, elevated TG2 transamidation due to increased intracellular calcium reportedly contributes to several dysfunctional cellular responses including altered vascular smooth muscle cell contractility in pulmonary hypertension and abnormal neurite outgrowth and differentiation in certain cognitive disorders [Guilluy et al., 2007; Dai et al., 2011]. In the GTP-bound state, TG2 appears to be resistant to calcium-activation of crosslinking. Accordingly, transamidation has been predominately viewed as an extracellular enzymatic reaction due to calcium excess outside the cell relative to available GTP [Begg et al., 2006]. Although cytosolic GTP levels also are in excess relative to calcium under normal physiological conditions, our results suggest that TG2-mediated transamidation of YB-1 substrate may be an advantaged reaction in TGFβ1-activated myofibroblasts. As an explanation, intracellular calcium levels in myofibroblasts may transiently exceed homeostatic levels in response to binding of fibrogenic agonists such as TGFβ1 and thrombin to their cognate receptors. Peroxide is known to activate TG2 transamidation and its

production as a direct consequence of TGFβ1 receptor-mediated induction of NADPH oxidase-4 activity in pulmonary fibroblasts could further enhance the accumulation of YB-1 oligomers [Griffith et al., 2009; Hecker et al., 2009]. TG2 transamidation also may be enabled by unknown ancillary factors that could mitigate GTP effects despite relatively high cytosolic GTP levels. For example, small GTP-binding proteins such as Rac1 associated with RhoA/Rho kinase (ROCK)-mediated regulation of actin filament assembly and myosin ATPase activation could alter the local intracellular GTP/GDP balance to favor increased TG2 transamidation [Russell et al., 2010]. Moreover, alternatively spliced TG2 isoforms have been identified that are not inhibited by GTP [Begg et al., 2006]. TG2 crosslinking reactions also might be spatially compartmentalized inside the cells and restricted to sites where calcium/GTP ratios are permissive for transamidation. The high calcium-buffering capacity of cytosol restricts calcium diffusion [Allbritton et al., 1992] resulting in the formation of microdomains where the local concentration of calcium can exceed that of bulk cytosol [Berridge, 2006].

Consistent with the notion of calcium-graded transamidation, we demonstrated that crosslinking of recombinant YB-1 by TG2 was calcium-concentration dependent. As little as 10–25 nM free calcium was capable of driving accumulation of p100-size variants that seemingly were rapidly converted into oligomers with apparent mass of 250 kDa or more. YB-1 size heterogeneity during SDS–PAGE also was evident in the vicinity of the p37–p50 size markers suggestive of TG2-mediated intra-molecular crosslinking and monomer isomerization possibly required as an intermediate step in the formation of high-molecular weight multimers. Others have suggested that TG2 crosslinking substrates may undergo isomerization prior to forming a glutamine substrate/acyl enzyme transition state [Case and Stein, 2003], an idea that is supported by the apparent size-shifting behavior of YB-1 p50 that was observed during the initial phase of the crosslinking reaction. YB-1 p50 size heterogeneity observed early during the transamidation reaction also may be related to altered access of YB-1 antibodies to epitope-binding sites and/or variable progression of transamidation due to changes in the ability of TG2 enzyme to access YB-1 substrate as it undergoes dynamic conformational changes within the reaction mixture. Calcium gradient-dependent regulation of TG2 transamidation is consistent with the well known spatial restriction of calcium in vivo, where levels in the cytosol are maintained approximately at 100 nM but may be much higher in the vicinity of calcium-release sites such as the endoplasmic reticulum (ER) when signaling intermediaries such as inositol-1,4,5-trisphosphate are formed in response to GPCR agonists. TG2-mediated transamidation of RhoA and Rac1 in vascular smooth muscle cells and neuronal cells recently was linked to ER-release of intracellular calcium stores [Guilluy et al., 2007; Dai et al., 2011]. We did not assess the ability of GTP to inhibit TG2-mediated crosslinking of YB-1. However, the low calcium threshold observed for in vitro crosslinking coupled with the observed formation of mRNA-binding YB-1 oligomers in intact cells suggests that a portion of the cytosolic YB-1 pool can be transamidated in response to accumulation of intracellular calcium and ROS expected as a natural consequence of the myofibroblast differentiation process.

Excessive TG2-mediated YB-1 oligomerization may represent a previously unrecognized mechanistic feature of interstitial and perivascular fibrosis and dysfunctional tissue remodeling in chronic cardiopulmonary disease. Interstitial fibrosis after cardiac transplant was accompanied by increased expression of myocardial SMαA as a consequence of cardiac myofibroblast activation, scar formation, and fetal contractile gene reprogramming in biomechanically stressed cardiomyocytes. YB-1 is a major SMαA mRNA-binding protein in myofibroblasts and reprogrammed cardiomyocytes and was prominently distributed in fibrotic heart grafts as both peri-nuclear granules and intense cytosolic deposits proximal to cardiac intercalated discs [Zhang et al., 2008; David et al., 2012]. Accumulation of YB-1 in heart grafts also has been linked to peri-transplant associated increases in TGFβ1 signaling and nuclear uptake of phosphorylated Smad proteins that drive fibrosis and dysfunctional remodeling in accepted heart grafts [Csencsits et al., 2006; Zhang et al., 2008]. Moreover, YB-1 localization at cardiac intercalated discs frequently was associated with de novo assembly of actin thin filaments that were highly enriched for SMαA. Of interest, YB-1 co-localized at intercalated discs with Pur α [Zhang et al., 2008], another prominent mRNA-binding protein in the heart and lung that mediates mRNA transport protein in neuronal cells through its ability to bind the kinesin microtubule motor protein [Ohashi et al., 2002; Kanai et al., 2004; Johnson et al., 2006; Aumiller et al., 2012; Strauch and Hariharan, 2013].

Data presented in this report suggests that SMαA mRNA may increase the rate and/or efficiency of YB-1 oligomer formation by calcium-activated TG2. Although the functional significance of this observation requires further analysis, we speculate that ribonucleoprotein complexes of YB-1 and mRNA may provide the physical means to selectively route pools of functionally related transcripts to polysomes for immediate protein synthesis. A viable scheme for translational control would require a mechanism for oligomer dispersion and release of SMαA mRNA payload. TG2-mediated reversal of covalent YB-1 cross linkages via cleavage of the isopeptide linkage with associated glutamine deamidation is a plausible mechanism for oligomer dissolution and release of YB-1-bound SMαA mRNA payload at cytosolic polysomes. We speculate that an intracellular pool of active TG2 with limited access to available lysine substrate in the YB-1 C-terminus would catalyze reversal of existing γ-glutamyl isopeptide links in YB-1 using water as the attacking nucleophile with subsequent release of glutamine-deamidated p50 YB-1. Compared to the nuclear fraction which is highly enriched for YB-1 size variants, preliminary cell fractionation analysis indicates that the myofibroblast cytosol contains a relatively smaller pool of YB-1 that might provide the YB-1-deficient milieu favorable for reversal of TG2-mediated crosslinks [Willis and Strauch, unpublished observations]. When transamidation is considered as a reversible process, TG2 may not only mediate calcium-regulated crosslinking of YB-1 and mRNA into storage granule structures but also enable their dissociation to permit rapid synthesis of selected proteins required for the wound-healing response. With respect to repairing tissue injury following heart transplant, mitochondria, the sodium/calcium exchanger, transient receptor potential channels, and the sarcoplasmic reticulum all are likely to be located peripherally near cardiac intercalated discs in metabolically stressed cardiomyocytes providing the necessary spatial compartmentalization for localizing reactive oxygen signaling intermediates and establishing calcium

microdomains [Eder and Molkentin, 2011]. In theory, calcium/ROS-mediated signaling would not only enable TG2 transamidation and YB-1 crosslinking but also could control the deamidation reaction required to unload mRNAs and re-program protein synthesis as needed in damaged tissue beds. TG2-mediated YB-1 crosslinking seems a plausible, testable mechanism for governing the stability, transport, and translational efficiency of multiple mRNA species required for normal myofibroblast differentiation and provides a novel target for therapeutic control of these cells to avoid unchecked fibrosis and dysfunctional cardiopulmonary remodeling.

ACKNOWLEDGEMENTS

The authors extend their gratitude to Professor Carl V. Leier, M.D. in the Division of Cardiovascular Medicine in the Ross Heart Hospital, Wexner Medical Center at The Ohio State University for the collection of endomyocardial biopsy specimens from heart transplant patients. This study was supported by NIH NHLBI grants HL 085109 and HL 110802 to A.R.S. Primary culture preparations of human pulmonary artery adventitial fibroblasts were provided by the University of Pennsylvania under the Pulmonary Hypertension Breakthrough Initiative (PHBI). Funding for the PHBI is provided by the Cardiovascular Medical Research and Education Fund (CMREF).

REFERENCES

Allbritton NL, Meyer T, Stryer L. 1992. Range of messenger action of calcium ion and inositol 1,4,5-trisphosphate. Science 258:1812–1815.

Anderson P. 2010. Post-transcriptional regulons coordinate the initiation and resolution of inflammation. Nat Rev Immunol 10:24–35.

Aumiller V, Graebsch A, Kremmer E, Niessing D, Forstemann K. 2012. Drosophila Pur-alpha binds to trinucleotide-repeat containing cellular RNAs and translocates to the early oocyte. RNA Biol 9:633–643.

Badarau E, Collighan RJ, Griffin M. 2013. Recent advances in the development of tissue transglutaminase (TG2) inhibitors. Amino Acids 44:119–127.

Becker NA, Kelm RJ, Jr., Vrana JA, Getz MJ, Maher LJI. 2000. Altered sensitivity to single-strand-specific reagents associated with the genomic vascular smooth muscle alpha-actin promoter during myofibroblast differentiation. J Biol Chem 275:15384–15391.

Begg GE, Carrington L, Stokes PH, Matthews JM, Wouters MA, Husain A, Lorand L, Iismaa SE, Graham RM. 2006. Mechanism of allosteric regulation of transglutaminase 2 by GTP. Proc Natl Acad Sci USA 103:19683–19688.

Berridge MJ. 2006. Calcium microdomains: Organization and function. Cell Calcium 40:405–412.

Bogatkevich GS, Tourkina E, Abrams CS, Harley RA, Silver RM, Ludwicka-Bradley A. 2003. Contractile activity and smooth muscle alpha-actin organization in thrombin-induced human lung myofibroblasts. Am J Physiol Lung Cell Mol Physiol 285:L334–L343.

Bogatkevich GS, Gustilo E, Oates JC, Feghali-Bostwick C, Harley RA, Silver RM, Ludwicka-Bradley A. 2005. Distinct PKC isoforms mediate cell survival and DNA synthesis in thrombin-induced myofibroblasts. Am J Physiol Lung Cell Mol Physiol 288:L190–L201.

Bondi CD, Manickam N, Lee DY, Block K, Gorin Y, Abboud HE, Barnes JL. 2010. NAD(P)H oxidase mediates TGF-beta1-induced activation of kidney myofibroblasts. J Am Soc Nephrol 21:93–102.

Bosc LVG, Layne JJ, Nelson MT, Hill-Eubanks DC. 2005. Nuclear factor of activated T cells and serum response factor cooperatively regulate the activity of an α-actin intronic enhancer. J Biol Chem 280:26113–26120.

Case A, Stein RL. 2003. Kinetic analysis of the action of tissue transglutaminase on peptide and protein substrates. Biochemistry 42:9466–9481.

Chernov KG, Curmi PA, Hamon L, Mechulam A, Ovchinnikov LP, Pastre D. 2008. Atomic force microscopy reveals binding of mRNA to microtubules mediated by two major mRNP proteins YB-1 and PABP. FEBS Lett 582: 2875–2881.

Chou CY, Streets AJ, Watson PF, Huang L, Verderio EA, Johnson TS. 2011. A crucial sequence for transglutaminase type 2 extracellular trafficking in renal tubular epithelial cells lies in its N-terminal beta-sandwich domain. J Biol Chem 286:27825–27835.

Cogan JG, Subramanian SV, Polikandriotis JA, Kelm RJ, Jr., Strauch AR. 2002. Vascular smooth muscle α-actin gene transcription during myofibroblast differentiation requires Sp1/3 protein binding proximal to the MCAT enhancer. J Biol Chem 277:36433–36442.

Coles LS, Bartley MA, Bert A, Hunter J, Polyak S, Diamond P, Vadas MA, Goodall GJ. 2004. A multi-protein complex containing cold shock domain (Y-box) and polypyrimidine tract binding proteins forms on the vascular endothelial growth factor mRNA. Potential role in mRNA stabilization. Eur J Biochem 271:648–660.

Csencsits K, Wood SC, Lu G, Faust SM, Brigstock D, Eichwald EJ, Orosz CG, Bishop DK. 2006. Transforming growth factor beta-induced connective tissue growth factor and chronic allograft rejection. Am J Transplant 6:959–966.

Csosz E, Bagossi P, Nagy Z, Dosztanyi Z, Simon I, Fesus L. 2008. Substrate preference of transglutaminase 2 revealed by logistic regression analysis and intrinsic disorder examination. J Mol Biol 383:390–402.

Dai Y, Dudek N, Li Q, Muma N. 2011. Phospholipase C, Ca2 +, and calmodulin signaling are required for 5-HT2A receptor-mediated transamidation of Rac1 by transglutaminase. Psychopharmacology 213:403–412.

David JJ, Subramanian SV, Zhang A, Willis WL, Kelm RJ, Leier CV, Strauch AR. 2012. Y-box binding protein-1 implicated in translational control of fetal myocardial gene expression after cardiac transplant. Exp Biol Med 237: 593–607.

Davis J, Burr A, Davis G, Birnbaumer L, Molkentin J. 2012. A TRPC6-dependent pathway for myofibroblast transdifferentiation and wound healing in vivo. Dev Cell 23:705–715.

Dooley S, Said HM, Gressner AM, Floege J, En-Nia A, Mertens PR. 2006. Y-box protein-1 is the crucial mediator of antifibrotic interferon-gamma effects. J Biol Chem 281:1784–1795.

Dweck D, Reyes-Alfonso A, Jr., Potter JD. 2005. Expanding the range of free calcium regulation in biological solutions. Anal Biochem 347:303–315.

Eder P, Molkentin JD. 2011. TRPC channels as effectors of cardiac hypertrophy. Circ Res 108:265–272.

Elberg G, Chen L, Elberg D, Chan MD, Logan CJ, Turman MA. 2008. MKL1 mediates TGFbeta1-induced alpha-smooth muscle actin expression in human renal epithelial cells. Am J Physiol Renal Physiol 294:F1116–F1128.

Eliseeva IA, Kim ER, Guryanov SG, Ovchinnikov LP, Lyabin DN. 2011. Y-box-binding protein 1 (YB-1) and its functions. Biochemistry (Mosc) 76: 1402–1433.

Evdokimova V, Ovchinnikov LP, Sorensen PH. 2006. Y-box binding protein 1: Providing a new angle on translational regulation. Cell Cycle 5: 1143–1147.

Frangogiannis NG. 2006. The mechanistic basis of infarct healing. Antioxid Redox Signal 8:1907–1939.

Fraser DJ, Phillips AO, Zhang X, van Roeyen CR, Muehlenberg P, En-Nia A, Mertens PR. 2008. Y-box protein-1 controls transforming growth factor-beta1 translation in proximal tubular cells. Kidney Int 73:724–732.

Gabbiani G. 2003. The myofibroblast in wound healing and fibrocontractive diseases. J Pathol 200:500–503.

Griffith B, Pendyala S, Hecker L, Lee PJ, Natarajan V, Thannickal VJ. 2009. NOX enzymes and pulmonary disease. Antioxid Redox Signal 11:2505–2516.

Grotendorst GR, Rahmanie H, Duncan MR. 2004. Combinatorial signaling pathways determine fibroblast proliferation and myofibroblast differentiation. FASEB J 18:469–479.

Guilluy C, Rolli-Derkinderen M, Tharaux PL, Melino G, Pacaud P, Loirand G. 2007. Transglutaminase-dependent RhoA activation and depletion by serotonin in vascular smooth muscle cells. J Biol Chem 282:2918–2928.

Gundemir S, Colak G, Tucholski J, Johnson GVW. 2012. Transglutaminase 2: A molecular Swiss army knife. Biochim Biophys Acta Mol Cell Res 1823: 406–419.

Hanssen L, Frye BC, Ostendorf T, Alidousty C, Djudjaj S, Boor P, Rauen T, Floege J, Mertens PR, Raffetseder U. 2011. Y-box binding protein-1 mediates profibrotic effects of calcineurin inhibitors in the kidney. J Immunol 187: 298–308.

Hecker L, Vittal R, Jones T, Jagirdar R, Luckhardt TR, Horowitz JC, Pennathur S, Martinez FJ, Thannickal VJ. 2009. NADPH oxidase-4 mediates myofibroblast activation and fibrogenic responses to lung injury. Nat Med 15: 1077–1081.

Higashi K, Inagaki Y, Fujimori K, Nakao A, Kaneko H, Nakatsuka I. 2003. Interferon-gamma interferes with transforming growth factor-beta signaling through direct interaction of YB-1 with Smad3. J Biol Chem 278:43470–43479.

Howell DC, Laurent GJ, Chambers RC. 2002. Role of thrombin and its major cellular receptor, protease-activated receptor-1, in pulmonary fibrosis. Biochem Soc Trans 30:211–216.

Ientile R, Caccamo D, Griffin M. 2007. Tissue transglutaminase and the stress response. Amino Acids 33:385–394.

Iismaa SE, Mearns BM, Lorand L, Graham RM. 2009. Transglutaminases and disease: Lessons from genetically engineered mouse models and inherited disorders. Physiol Rev 89:991–1023.

Jeon JH, Lee HJ, Jang GY, Kim CW, Shim DM, Cho SY, Yeo EJ, Park SC, Kim IG. 2004. Different inhibition characteristics of intracellular transglutaminase activity by cystamine and cysteamine. Exp Mol Med 36:576–581.

Johnson EM, Kinoshita Y, Weinreb DB, Wortman MJ, Simon R, Khalili K, Winckler B, Gordon J. 2006. Role of Pur alpha in targeting mRNA to sites of translation in hippocampal neuronal dendrites. J Neurosci Res 83:929–943.

Kanai Y, Dohmae N, Hirokawa N. 2004. Kinesin transports RNA: Isolation and characterization of an RNA-transporting granule. Neuron 43:513–525.

Keene JD. 2007. RNA regulons: Coordination of post-transcriptional events. Nat Rev Genet 8:533–543.

Kelm RJ, Jr., Cogan JG, Elder PK, Strauch AR, Getz MJ. 1999a. Molecular interactions between single-stranded DNA-binding proteins associated with all essential MCAT element in the mouse smooth muscle α-actin promoter. J Biol Chem 274:14238–14245.

Kelm RJ, Jr., Elder PK, Getz MJ. 1999b. The single-stranded DNA-binding proteins, Purα, Purβ, and MSY1 specifically interact with an exon 3-derived mouse vascular smooth muscle α-actin messenger RNA sequence. J Biol Chem 274:38268–38275.

Keresztessy Z, Csosz E, Harsfalvi J, Csomos K, Gray J, Lightowlers RN, Lakey JH, Balajthy Z, Fesus L. 2006. Phage display selection of efficient glutamine-donor substrate peptides for transglutaminase 2. Protein Sci 15:2466–2480.

Kiraly R, Csosz E, Kurtan T, Antus S, Szigeti K, Simon-Vecsei Z, Korponay-Szabo IR, Keresztessy Z, Fesus L. 2009. Functional significance of five noncanonical Ca2+-binding sites of human transglutaminase 2 characterized by site-directed mutagenesis. FEBS J 276:7083–7096.

Knapp AM, Ramsey JE, Wang SX, Godburn KE, Strauch AR, Kelm RJ, Jr. 2006. Nucleoprotein interactions governing cell type-dependent repression of the mouse smooth muscle alpha-actin promoter by single-stranded DNA-binding proteins Pur alpha and Pur beta. J Biol Chem 281:7907–7918.

Kohno K, Izumi H, Uchiumi T, Ashizuka M, Kuwano M. 2003. The pleiotropic functions of the Y-box-binding protein, YB-1. Bioessays 25:691–698.

Kojima S, Nara K, Rifkin DB. 1993. Requirement for transglutaminase in the activation of latent transforming growth factor-beta in bovine endothelial cells. J Cell Biol 121:439–448.

Kuo TF, Tatsukawa H, Kojima S. 2011. New insights into the functions and localization of nuclear transglutaminase 2. FEBS J 278:4756–4767.

Kuroda J, Ago T, Matsushima S, Zhai P, Schneider MD, Sadoshima J. 2010. NADPH oxidase 4 (Nox4) is a major source of oxidative stress in the failing heart. Proc Natl Acad Sci USA 107:15565–15570.

Lin CY, Tsai PH, Kandaswami CC, Chang GD, Cheng CH, Huang CJ, Lee PP, Hwang JJ, Lee MT. 2011. Role of tissue transglutaminase 2 in the acquisition of a mesenchymal-like phenotype in highly invasive A431 tumor cells. Mol Cancer 10:87–97.

Liu X, Kelm RJ, Jr., Strauch AR. 2009. Transforming growth factor beta1-mediated activation of the smooth muscle alpha-actin gene in human pulmonary myofibroblasts is inhibited by tumor necrosis factor-alpha via mitogen-activated protein kinase kinase 1-dependent induction of the Egr-1 transcriptional repressor. Mol Biol Cell 20:2174–2185.

Mann AP, Verma A, Sethi G, Manavathi B, Wang H, Fok JY, Kunnumakkara AB, Kumar R, Aggarwal BB, Mehta K. 2006. Overexpression of tissue transglutaminase leads to constitutive activation of nuclear factor-kappaB in cancer cells: Delineation of a novel pathway. Cancer Res 66:8788–8795.

Masszi A, Speight P, Charbonney E, Lodyga M, Nakano H, Szaszi K, Kapus A. 2010. Fate-determining mechanisms in epithelial-myofibroblast transition: Major inhibitory role for Smad3. J Cell Biol 188:383–399.

Mehta K, Kumar A, Kim HI. 2010. Transglutaminase 2: A multi-tasking protein in the complex circuitry of inflammation and cancer. Biochem Pharmacol 80:1921–1929.

Meoli DF, White RJ. 2009. Thrombin induces fibronectin-specific migration of pulmonary microvascular endothelial cells: Requirement of calcium/calmodulin-dependent protein kinase II. Am J Physiol Lung Cell Mol Physiol 297: L706–L714.

Mishra S, Murphy LJ. 2006. The p53 oncoprotein is a substrate for tissue transglutaminase kinase activity. Biochem Biophys Res Commun 339:726–730.

Murthy SN, Lukas TJ, Jardetzky TS, Lorand L. 2009. Selectivity in the post-translational, transglutaminase-dependent acylation of lysine residues. Biochemistry 48:2654–2660.

Nekrasov MP, Ivshina MP, Chernov KG, Kovrigina EA, Evdokimova VM, Thomas AA, Hershey JW, Ovchinnikov LP. 2003. The mRNA-binding protein YB-1 (p50) prevents association of the eukaryotic initiation factor eIF4G with mRNA and inhibits protein synthesis at the initiation stage. J Biol Chem 278:13936–13943.

Nishida M, Onohara N, Sato Y, Suda R, Ogushi M, Tanabe S, Inoue R, Mori Y, Kurose H. 2007. Gα12/13-mediated up-regulation of TRPC6 negatively regulates endothelin-1-induced cardiac myofibroblast formation and collagen synthesis through nuclear factor of activated T cells activation. J Biol Chem 282:23117–23128.

Norman JT, Lindahl GE, Shakib K, En-Nia A, Yilmaz E, Mertens PR. 2001. The Y-box binding protein YB-1 suppresses collagen alpha 1(I) gene transcription via an evolutionarily conserved regulatory element in the proximal promoter. J Biol Chem 276:29880–29890.

O'Donnell BV, Tew DG, Jones OT, England PJ. 1993. Studies on the inhibitory mechanism of iodonium compounds with special reference to neutrophil NADPH oxidase. Biochem J 290:41–49.

Oh K, Park HB, Byoun OJ, Shin DM, Jeong EM, Kim YW, Kim YS, Melino G, Kim IG, Lee DS. 2011. Epithelial transglutaminase 2 is needed for T cell interleukin-17 production and subsequent pulmonary inflammation and fibrosis in bleomycin-treated mice. J Exp Med 208:1707–1719.

Ohashi S, Koike K, Omori A, Ichinose S, Ohara S, Kobayashi S, Sato TA, Anzai K. 2002. Identification of mRNA/protein (mRNP) complexes containing Puralpha, mStaufen, fragile X protein, and myosin Va and their association

with rough endoplasmic reticulum equipped with a kinesin motor. J Biol Chem 277:37804–37810.

Olsen KC, Sapinoro RE, Kottmann RM, Kulkarni AA, Iismaa SE, Johnson GV, Thatcher TH, Phipps RP, Sime PJ. 2011. Transglutaminase 2 and its role in pulmonary fibrosis. Am J Respir Crit Care Med 184:699–707.

Onishi H, Kino Y, Morita T, Futai E, Sasagawa N, Ishiura S. 2008. MBNL1 associates with YB-1 in cytoplasmic stress granules. J Neurosci Res 86:1994–2002.

Park D, Choi SS, Ha KS. 2010. Transglutaminase 2: A multi-functional protein in multiple subcellular compartments. Amino Acids 39:619–631.

Russell B, Curtis MW, Koshman YE, Samarel AM. 2010. Mechanical stress-induced sarcomere assembly for cardiac muscle growth in length and width. J Mol Cell Cardiol 48:817–823.

Sabri A, Short J, Guo J, Steinberg SF. 2002. Protease-activated receptor-1-mediated DNA synthesis in cardiac fibroblast is via epidermal growth factor receptor transactivation: Distinct PAR-1 signaling pathways in cardiac fibroblasts and cardiomyocytes. Circ Res 91:532–539.

Santhanam L, Tuday EC, Webb AK, Dowzicky P, Kim JH, Oh YJ, Sikka G, Kuo M, Halushka MK, Macgregor AM, Dunn J, Gutbrod S, Yin D, Shoukas A, Nyhan D, Flavahan NA, Belkin AM, Berkowitz DE. 2010. Decreased S-nitrosylation of tissue transglutaminase contributes to age-related increases in vascular stiffness. Circ Res 107:117–125.

Selivanova OM, Guryanov SG, Enin GA, Skabkin MA, Ovchinnikov LP, Serdyuk IN. 2010. YB-1 is capable of forming extended nanofibrils. Biochemistry (Mosc) 75:115–120.

Skabkin MA, Kiselyova OI, Chernov KG, Sorokin AV, Dubrovin EV, Yaminsky IV, Vasiliev VD, Ovchinnikov LP. 2004. Structural organization of mRNA complexes with major core mRNP protein YB-1. Nucleic Acids Res 32:5621–5635.

Small EM, Thatcher JE, Sutherland LB, Kinoshita H, Gerard RD, Richardson JA, DiMaio JM, Sadek H, Kuwahara K, Olson EN. 2010. Myocardin-related transcription factor-A controls myofibroblast activation and fibrosis in response to myocardial infarction. Circ Res 107:294–304.

Snead AN, Insel PA. 2012. Defining the cellular repertoire of GPCRs identifies a profibrotic role for the most highly expressed receptor, protease-activated receptor 1, in cardiac fibroblasts. FASEB J 26:4540–4547.

Stamnaes J, Fleckenstein B, Sollid LM. 2008. The propensity for deamidation and transamidation of peptides by transglutaminase 2 is dependent on substrate affinity and reaction conditions. Biochim Biophys Acta 1784:1804–1811.

Stamnaes J, Pinkas DM, Fleckenstein B, Khosla C, Sollid LM. 2010. Redox regulation of transglutaminase 2 activity. J Biol Chem 285:25402–25409.

Stephens P, Grenard P, Aeschlimann P, Langley M, Blain E, Errington R, Kipling D, Thomas D, Aeschlimann D. 2004. Crosslinking and G-protein functions of transglutaminase 2 contribute differentially to fibroblast wound healing responses. J Cell Sci 117:3389–3403.

Strauch AR, Hariharan S. 2013. Dynamic interplay of smooth muscle α-actin gene regulatory proteins reflects the biological complexity of myofibroblast differentiation. Biology (MDPI, Basel) 2:555–586.

Subramanian SV, Kelm RJ, Jr., Polikandriotis JA, Orosz CG, Strauch AR. 2002. Reprogramming of vascular smooth muscle alpha-actin gene expression as an early indicator of dysfunctional remodeling following heart transplant. Cardiovasc Res 54:539–548.

Subramanian SV, Polikandriotis JA, Kelm RJJ, David JJ, Orosz CG, Strauch AR. 2004. Induction of vascular smooth muscle alpha-actin gene transcription in transforming growth factor beta1-activated myofibroblasts mediated by dynamic interplay between the Pur repressor proteins and Sp1/Smad coactivators. Mol Biol Cell 15:4532–4543.

Telci D, Collighan RJ, Basaga H, Griffin M. 2009. Increased TG2 expression can result in induction of transforming growth factor beta1, causing increased synthesis and deposition of matrix proteins, which can be regulated by nitric oxide. J Biol Chem 284:29547–29558.

Willis BC, Borok Z. 2007. TGF-beta induced EMT: Mechanisms and implications for fibrotic lung disease. Am J Physiol Lung Cell Mol Physiol 293:L525–L534.

Wolffe AP. 1994. Structural and functional properties of the evolutionarily ancient Y-box family of nucleic acid binding proteins. BioEssays 16: 245–251.

Yamasaki S, Anderson P. 2008. Reprogramming mRNA translation during stress. Curr Opin Cell Biol 20:222–226.

Yang WH, Bloch DB. 2007. Probing the mRNA processing body using protein macroarrays and "autoantigenomics". RNA 13:704–712.

Zhang A, Liu X, Cogan JG, Fuerst MD, Polikandriotis JA, Kelm RJJ, Strauch AR. 2005. YB-1 coordinates vascular smooth muscle alpha-actin gene activation by TGFbeta1 and thrombin during differentiation of human pulmonary myofibroblasts. Mol Biol Cell 16:4931–4940.

Zhang A, David JJ, Subramanian SV, Liu X, Fuerst MD, Zhao X, Leier CV, Orosz CG, Kelm RJ, Jr., Strauch AR. 2008. Serum response factor neutralizes Pur alpha- and Pur beta-mediated repression of the fetal vascular smooth muscle alpha-actin gene in stressed adult cardiomyocytes. Am. J. Physiol Cell Physiol 294:C702–C714.